

Metalloproteinase-9 contributes to inflammatory glia activation and nigro-striatal pathway degeneration in both mouse and monkey models of 1-methyl-4-phenyl-1,2,3,6-tetrahydropyridine (MPTP)- induced Parkinsonism

Annese V.^{1,4}, Herrero M.T.^{3,4} Di Pentima M.¹, Gomez A.⁴, Lombardi L.¹, Ros C.M.^{3,4}, De Pablos V.⁴, Fernandez-Villalba E.⁴ and De Stefano M.E.^{1,2}

¹Istituto Pasteur-Fondazione Cenci Bolognetti, Dipartimento di Biologia e Biotecnologie “Charles Darwin” and ²Center for Research in Neurobiology “Daniel Bovet”, Sapienza Università di Roma, 00185 Roma, Italy; ³School of Health Sciences (Medicine), University Jaume I, 12071 Castelló de la Plana, Spain; ⁴Clinical & Experimental Neuroscience (NiCE-CIBERNED), School of Medicine, University of Murcia, 30100 Murcia, Spain

Corresponding authors:

Maria Egle De Stefano
Dipartimento di Biologia e Biotecnologie “Charles Darwin”
Sapienza Università di Roma
P.le Aldo Moro 5
00185 Roma - Italy
Tel: 011-39-06-49912230
Fax:011-39-06-49912351
e-mail: egle.destefano@uniroma1.it

María-Trinidad Herrero Ezquerro
Clinical and Experimental Neuroscience (NiCE-CIBERNED)
School of Health Sciences (Medicine)
University Jaume I, 12071
Castelló de la Plana, Spain.
Tel: 00-34-964-387459
Fax: 00-34-964-729016
Email: ezquerro@uji.es

Running Title: MMP-9 in Parkinsonism-associated neuroinflammation

ABSTRACT

Inflammation is a predominant aspect of neurodegenerative diseases, and is manifested by glia activation and expression of pro-inflammatory mediators. Studies on animal models of Parkinson's disease (PD) suggest that sustained neuroinflammation exacerbates degeneration of the dopaminergic (DA) nigro-striatal pathway. Therefore, insights into the inflammatory mechanisms of PD may help the development of novel therapeutic strategies against this disease. As extracellular matrix metalloproteinases (MMPs) could be major players in the progression of Parkinsonism, we investigated, in the substantia nigra (SN) and striatum of mice acutely injected with 1-methyl-4-phenyl-1,2,3,6-tetrahydropyridine (MPTP), changes in mRNA expression, protein levels, and cell localization of MMP-9. This protease is mainly neuronal, but early after MPTP injection its mRNA and protein levels, as well as the number of MMP-9-expressing microglia and astrocytes, increase concomitantly to a prominent inflammation. Neuroinflammation and MMP-9⁺ glia begin to decline within 2 weeks, although protein levels remain higher than control, in association with a partial recovery of DA nigro-striatal circuit. Comparable quantitative studies on MMP-9 knock-out mice, show a significant decrease in both glia activation and loss of DA neurons and fibers, with respect to wild-type. Moreover, in a parallel study on chronically MPTP-injected macaques, we observed that perpetuation of inflammation and high levels of MMP-9 are associated to DA neuron loss. Our data suggest that MMP-9 released by injured neurons favors glia activation; glial cells in turn reinforce their reactive state *via* autocrine MMP-9 release, contributing to nigro-striatal pathway degeneration. Specific modulation of MMP-9 activity may, therefore, be a strategy to ameliorate harmful inflammatory outcomes in Parkinsonism.

Key words: Metalloproteinases; Neuroinflammation; Parkinson's disease; Neurodegeneration.

INTRODUCTION

Parkinson's disease (PD) is a neurodegenerative disorder characterized by progressive loss of dopaminergic (DA) neurons in the substantia nigra *pars compacta* (SN_{pc}) (Hirsch et al. 1988; Braak et al. 2003, 2006). Idiopathic PD affects mainly the elderly, but it can also develop in young people, where a genetic component may play a prominent role (Houlden and Singleton 2012). The etiology of this disease remains to be elucidated; however, as PD is characterized by a prominent inflammatory reaction, which becomes chronic along the years, neuroinflammation may play a role in exacerbation (Hirsch and Hunot 2009; Tansey and Goldberg 2010), or even promotion (Whitton 2010), of the disease. *Post-mortem* analysis (McGeer et al. 1988; Hirsch et al. 1998; Ouchi et al. 2005, 2009; Braak et al. 2007) and *in vivo* imaging (Ouchi et al. 2005, 2009; Gerard et al. 2006) of PD patient brains showed activation of microglia, astrogliosis and infiltration of peripheral immune cells in the SN_{pc} and other regions. These features were also observed in the brain of young drug addicts, who made use of the neurotoxin 1-methyl-4-phenyl-1,2,3,6-tetrahydropyridine (MPTP) (Langston et al. 1983), and in animal models of Parkinsonism, such as MPTP-injected mice and monkeys (Barnum and Tansey 2010; Walsh et al. 2011). Increased levels of pro-inflammatory cytokines in both SN (Hunot et al. 1996; Hirsch et al. 1998; Barcia et al. 2005, 2011) and cerebrospinal fluid (Nagatsu et al. 2000; Pott Godoy et al. 2008) of PD patients and animal models have also been described. The complexity of the immune response, however, does not allow to unequivocally establish whether reactive "neuroglia" contributes to DA neuron death. Anti-inflammatory therapies are used in the treatment of a number of neurodegenerative disorders, including PD (Whitton 2010; L'Episcopo et al. 2010); however, from a drug-development perspective, a complete understanding of the factors and mechanisms ruling the onset and progression of disease-specific inflammatory processes is most needed. An intriguing idea is that glial cells may play important and diverse roles during the progression of the disease, a critical moment being the switch from acute to chronic inflammation.

Matrix metalloproteinases (MMPs) are extracellular proteases that finely modulate several

physiological and pathological/inflammatory processes (Parks et al. 2004; Page-McCaw et al. 2007; Candelario-Jalil et al. 2009; Wright and Harding 2009). MMP-2 and -9 are highly expressed in the brain in physiological conditions, and MMP-9 and -3 are significantly up-regulated in several brain pathologies, including PD (Lorenzl et al. 2002, Kim et al. 2007, 2011; Choi et al. 2008), highlighting them as possible therapeutic targets (Leonardo and Pennypacker 2009). Specific MMP inhibitors have been developed; however, indiscriminate block of this enzymatic activity is a dangerous ground, since MMPs play different roles depending on the type of pathology and time of activation.

In this study we investigated changes in MMP-9 expression and localization in the MPTP mouse and monkey models of Parkinsonism. Our results indicate that: 1) MMP-9 is important for inflammatory glia activation, which in turn exacerbates DA neuron loss; 2) at later stages, when neuroinflammation subsides, MMP-9 may contribute to partial recovery of the nigro-striatal pathway.

MATERIALS AND METHODS

All studies were carried out in accordance with the guidelines promulgated in the National Institutes of Health Guide for the Care and Use of Laboratory Animals (NIH Guide, revised 1996), in the European Convention for the protection of Vertebrate Animals used for Experimental and other scientific purposes of the Council of Europe (no 123, June 15th, 2006), and in accordance with The Code of Ethics of the EU Directive 2010/63/EU. All efforts were made to minimize animal suffering, to reduce the number of animals used, and to utilize alternatives to *in vivo* techniques. The experimental procedures and protocols were approved by the Ethical Committee for Animal Research of the University of Murcia and of the Italian Ministry of Public Health.

MPTP treatment

Mice. We used three month-old male C57BL/6J mice, B6.FVB(Cg)-*Mmp9*^{tm1Tvu}/J mice and their matching wild-type (WT) mice (The Jackson Laboratory, Bar Harbor, MA, USA). Mice were housed in a separate room, at 21 °C, under a 12 hours (h) day-night cycle and with food and water *ad libitum*. Acute MPTP treatment was performed according to established protocols (Jackson-Lewis et al. 1995). Briefly, mice received four intra-peritoneal (i.p.) injections of 20 mg/kg of MPTP·HCl (Sigma-Aldrich, St. Louis, MO, USA) dissolved in 0.9 % NaCl at 2 h intervals. We always used freshly diluted MPTP and adopted special animal care (i.e. warm room temperature and cages provided with cotton wool) in order to minimize mice loss after treatment. Only 5 mice over the total used (see details below) died after MPTP injection. Control mice received equivalent injections of saline. The number of mice used was: for molecular biology and biochemical studies, 8 mice/experimental group and type of analyses, for a total of 112 mice (56 mice each); for confocal analyses, 4 mice/experimental group, for a total of 20 mice; for immunohistochemistry, 5 WT mice/experimental point and 8 MMP-9 KO mice/experimental group, for a total of 15 WT and 24 MMP-9 KO mice, respectively. Mice were killed at established time points (see specific paragraphs) and brains removed and processed for different analysis.

Macaques. Brain sections were derived from a colony of chronic parkinsonian macaques (*Macaca fascicularis*) previously established and studied at the Primate Unit of the University of Murcia, and were properly stored. Samples were obtained from six young adult macaques, four of which had been treated weekly with low intravenous doses of MPTP (0.3 mg/kg) until stable Parkinsonism was established (Herrero et al. 1993; Barcia et al. 2003). This varied, depending on individual susceptibility to the toxin. Progressive motor alterations were assessed using a rating scale ranging from 0 to 25 (Herrero et al. 1993) (Table 1). Parkinsonian macaques were sacrificed 2 years after the last MPTP administration. Monkeys not treated with MPTP were used as controls. For this study, three control and 5 parkinsonian macaques were used.

Real Time Reverse Transcriptase-Polymerase Chain Reaction

mRNA levels of MMP-9 were assessed in the brain of control and MPTP-treated C57BL/6J mice by Real Time Reverse transcriptase-Polymerase Chain Reaction (RT-PCR). Animals were deeply anesthetized with isoflurane (Merial, Harlow, UK) and killed by decapitation at different time points after the last MPTP injection: 1 h, 24 h, 48 h, 72 h, 1 week (w) and 2 w. Brains were rapidly removed, frozen in liquid nitrogen-cooled isopentane, and stored at -80 °C until use. Frozen brains were cut in 1 mm-thick coronal sections on a matrix for brain slicing (AgnTho's, Lidingö, Sweden), and dorsal striatum and SN were removed by excision with a thin needle and a punching device of 0.75 mm of internal diameter (AgnTho's), respectively. Samples were rapidly homogenized for RNA extraction.

RNA extraction, quantification and reverse transcription

Total RNA was isolated from SN and striatum of control and MPTP-treated C57BL/6J mice using the RNeasy Micro kit (Qiagen, Milan, Italy) according to the manufacturer's instructions. RNA was purified from genomic DNA by using the DNA-free kit (Ambion, Austin, TX, USA), and quantity and purity was assessed by the Nanodrop ND-1000 spectrophotometer at 260 nm. RNA integrity was assessed by electrophoresis on ethidium bromide-stained 1 % agarose-formaldehyde gels. RNA was

reverse-transcribed as previously described (Del Signore et al., 2006) by using the cDNA synthesis kit (Bioline, London, UK). cDNA samples were stored at -20 °C until use.

Real time RT-PCR

2.5 µl of cDNA were amplified by real time RT-PCR in 25 µl of a reaction mixture containing 12.5 µl of 2 X SYBR Green JumpStart Taq ReadyMix (Sigma-Aldrich), 0.25 µl of Internal Reference Dye and 3 µl of each specific primer (5 µM final concentration Forward + Reverse) (Sigma-Aldrich), by using an iCycler iQ Real-Time Detection System (Bio-Rad, Milan, Italy). Each sample was amplified in duplicate for 30-35 cycles. Amplicons were detected after each elongation step and analyzed using the iCycler iQ software (Bio-Rad). A melting curve was obtained after completion of the cycles to verify the presence of a single amplified product. Relative quantification was carried out with the $2^{-\Delta\Delta C_t}$ method (Livak and Schmittgen 2001), using the abundance of hypoxanthinephospho-ribosyl-transferase (HPRT) as endogenous house-keeping control. The specificity of each pair of primers was confirmed by comparing to a negative control with water. Primers used were the following:

MMP-9 F, 5'-GGCGTGTCTGGAGATTCG-3', R, 5'-ATGGCAGAAATAGGCTTTGTC-3';

HPRT F, 5'- AGTCCCAGCGTCGTGATTAG-3', R, 5'- CCATCTCCTTCATGACATCTCG-3'

Western immunoblot

Primary antibodies

Rabbit polyclonal antibodies against MMP-9 (1:2000) and tyrosine hydroxylase (TH) (1:1000) were from Chemicon (Temecula, CA, USA). Mouse monoclonal antibody against glyceraldehyde phosphate dehydrogenase (GAPDH, 1:5000) was from Abcam (Cambridge, UK).

Preparation of tissue extracts, electrophoresis and immunoblotting

Time periods of MPTP treatment and tissue preparation from control and MPTP-treated C57BL/6J mice were as described for real time RT-PCR. Tissues were homogenized with a ground-glass micro-homogenizer in ice-cold RIPA buffer (50 mM Tris/HCl pH 7.6, 150 mM NaCl, 1 mM

EDTA, 1 % SDS, 1 % Triton X-100, 1X of a cocktail of inhibitors, 1 mM PMSF, 0.2 mM Na₃VO₄ and 1 mM NaF). After centrifugation (15000 x g, 15 min at 4 °C), a measured volume of supernatant was analyzed to determine total protein concentration using the Micro BCA kit (Pierce, Rockford, IL, USA). Other aliquots of the supernatant were diluted with 4X reducing loading buffer (200 mM Tris/HCl pH 6.8, 4 % SDS, 30 % glycerol, 4 % β-mercaptoethanol, 4 % blue bromophenol), boiled for 3 min at 100 °C, and stored at -20 °C until use.

Eighty micrograms of proteins of each sample were separated on 8 % SDS-polyacrylamide gels. Loading of such a high amount of proteins was necessary to obtain a proper densitometric signal, as the levels of MMP-9 in SN and striatum from a single mouse are too low with respect to total protein content. Molecular mass standard (ColorBurst®, Sigma-Aldrich), containing precisely sized recombinant proteins of 210, 90, 65, 40, 30, 20, 13 and 8 KDa, along with human recombinant gelatinases MMP-9 and MMP-2 (used as positive controls), were loaded on separate lanes next to the specimen homogenates. Gels were run at a constant 200 V, proteins transferred overnight onto a nitrocellulose membrane (transfer buffer: 50 mM Tris/HCl, 380 mM glycine, 0.1 % SDS and 20 % methanol) and correct electrophoretic migration and uniform protein loading was verified by Ponceau S staining (Biorad). Non-specific binding sites were blocked in 5 % dry milk (DM) (Carnation instant no-fat milk, Nestlé, USA), diluted in 1X TBST (20 mM Tris/HCl pH 7.5, 500 mM NaCl, 0.05 % Tween-20) (2 h at RT). Membranes were successively incubated (overnight at 4 °C) with the primary antibodies (diluted in 3 % BSA, 0.05 % NaN₃, 1X TBST) and then (1 h at RT) with the appropriate horseradish peroxidase (HRP)-conjugated secondary antibody (Promega, Madison, WI, USA): goat anti-rabbit IgG or goat anti-mouse IgG, diluted 1:10000 and 1:15000, respectively, in 2.5 % dry milk, 1X TBST. Antibody binding sites were revealed by using an enhanced chemiluminescence (ECL) kit (Pierce, Rockford, IL, USA) and exposing membranes to the Hyperfilm ECL (GE Healthcare, Waukesha, WI, USA). Densitometric analysis of the immunopositive bands was performed by using the ImageQuant 5.2 software (GE Healthcare). The optical density (O.D.) of each band, expressed as arbitrary gray units, was normalized against the

O.D. of the GAPDH-positive band in the same lane, used as the internal reference protein. Densitometric values were expressed as the ratio of O.D. between MPTP and control mice.

In situ zymography

Gelatinolytic activity (MMP-9 and MMP-2) in SN_{pc} and striatum of control and MPTP-treated (72 h) C57BL/6J mice was evaluated by *in situ* zymography on frozen brain sections. Animals were anesthetized with isoflurane and killed by decapitation, brains were rapidly removed, frozen on dry-ice and stored at -80 °C until use. Coronal serial sections (10 µm-thick) were cut at a cryostat, mounted on Super Frost Ultra Plus® glass slides (Menzel-Gläser, Braunschweig, Germany) and incubated overnight at 37 °C in a gelatinase activation buffer composed by 50 mM Tris/HCl (pH 7.6), 150 mM NaCl, 5 mM CaCl₂, 0.2 mM NaN₃ e 50 µg/ml of DQ™ Gelatin from Pig Skin Fluorescein-Conjugated (Molecular Probes, Eugene, OR, USA). Negative controls were obtained by adding 20 mM EDTA to the activation buffer. Before being coverslipped with Prolong® Gold antifade reagent (Invitrogen), sections were post-fixed (30 min at RT) with 4 % formalin in phosphate buffered saline (PBS) and nuclei counterstained with diamidino-2-phenylindole (DAPI) (1:1000, Invitrogen). Sites of proteolytic activities, visible as a fluorescent emission consequent to gelatin enzymatic cleavage by MMPs, were observed with a Zeiss Axioplan 2 microscope.

Immunohistochemistry, immunofluorescence and confocal analysis

Primary antibodies

Sheep anti-TH (1:1000), mouse anti-NeuN (1:500), mouse anti-glial fibrillary acid protein (GFAP, 1:500) and rabbit anti-MMP-9 (1:1000) were from Chemicon. Rabbit anti-Iba-1 (1:500) was from Wako (Chuo-Ku, Osaka, Japan).

Animal treatment

Mice. C57BL/6J mice, B6.FVB(Cg)-*Mmp9*^{tm1^{Tvu}/J} mice, and their matching WT mice were deeply anesthetized with an i.p. injection of Ketamine (50 mg/kg body weight) and Xylazine (50 mg/kg body weight), and perfused transcardially with an oxygenated Ringer solution (pH 7.3), followed by

4 % freshly depolymerized paraformaldehyde (PFA) in 0.1 M phosphate buffer (PB) (pH 7.4). Brains were removed and cryoprotected in 30 % sucrose, at 4 °C, until they sank. Free-floating coronal serial sections (25 µm-thick) were cut at a cryostat and stored in cryoprotectant (ethylene glycol : 0.2 M PB, pH 7.4 in a 1:1 proportion, with addition of 0.5 M sucrose) at -20 °C until use. Experimental groups and times after MPTP treatment were the following: C57BL/6J (control, 24 h, 48 h, 72 h, 1 w and 2 w after MPTP injection), B6.FVB(Cg)-*Mmp9^{tm1Tvu}*/J mice and their matching WT (control, 72 h and 2 w after MPTP injection).

Macaques. Macaques were killed by a lethal injection of pentobarbital after a pre-anesthesia with ketamine (8 mg/kg body weight). Brains were rapidly removed, fixed for 3 days in 4 % freshly depolymerized PFA in 0.1 M PB (pH 7.4) and sectioned into coronal 40 µm-thick serial sections at a vibratome (Barcia et al. 2004).

Immunofluorescence

Localization of MMP-9 by immunofluorescence was enhanced by using the Renaissance® Tyramide Signal Amplification (TSA)-biotin system kit (PerkinElmer), according to the manufacturer's instructions. After antigen retrieval with citrate buffer (pH 6.0) (30 min at 65 °C) and quenching of the endogenous peroxidase activity, sections were incubated (1 h at RT) in a TNB blocking buffer (0.1 M Tris/HCl pH 7.5, 0.15 M NaCl, 0.5 % blocking reagent by the manufacturer) and then (48 h at 4 °C) with the rabbit anti-MMP-9 antibody in combination with one of the other primary antibodies (see above), diluted in TNB blocking buffer. Amplification of the signal was obtained by incubation (30 min at RT) with a biotinylated goat anti-rabbit IgG secondary antibody (1:100, Vector Labs, Burlingame, CA, USA), diluted in TNB blocking buffer, followed by streptavidin–HRP conjugate (SA-HRP) (1:100, 30 min at RT), and finally by a biotinyl tyramide working solution (1:50 Biotinyl Tyramide Stock Solution diluted in 1X Amplification Diluent, 10 min at RT). Amplification was blocked by rinsing the sections in TNT buffer, and antibody-antigen binding sites were revealed by a 30 min incubation in the SA-Fluorescein conjugate (1:500 in TNB), followed by the appropriate secondary antibody conjugated with either Alexa Fluor 633 or

Alexa Fluor 594 (1:1000) (Molecular Probes, Carlsbad, CA, USA). DAPI was used for nuclear staining and sections were collected on glass slides and coverslipped with the Prolong® Gold reagent.

In mice, presence of MMP-9 in microglial cells was ascertained by MMP-9 immunolabeling followed by a staining with the widely used rhodamine-conjugated tomato lectin, *Griffonia Simplicifolia* Lectin I (GSA) (Vector Labs) diluted 1:100 (Pott Godoy et al., 2008).

Confocal analysis

Fluorescent specimens were viewed under a Leica DMIRE2 confocal microscope (Leica Microsystems, Wetzlar, Germany) with a 63X immersion-oil objective, except for the MMP-9/tomato lectin localization, which was analyzed at the Zeiss Axioplan 2 microscope, as fluorescence faded rapidly under the laser beam. Acquired images were analyzed with the Leica Confocal Software. To avoid cross talk between the fluorophores, we carefully adjusted the spectral ranges of detectors and scanned images sequentially. Each section was scanned in 0.5 µm-thick optical sections, the series range being determined by setting the upper and the lower thresholds with the Z/Y Position for Spatial Image Series setting. Images are presented as a transparency of all layers merged together. For further details see Barcia et al. (2008).

Immunohistochemistry

Endogenous peroxidase was inhibited (0.3 % H₂O₂ and 10 % methanol in PBS, for 15 min at RT) and then antigen retrieval was performed as described above. After a pre-permeabilization with 1 % Triton X-100, non-specific antibody binding sites were blocked in 10 % normal horse serum (NHS) in 0.1 M PBS (60 min at RT), and then slices were incubated (48 h, at 4 °C) with the anti-TH primary antibody, diluted in 1 % NHS, 0.5 % Triton X-100, 0.1 % NaN₃ and PBS, followed by a biotinylated donkey anti-sheep IgG (Jackson Immuno Research) (1:500, for 2 h), and then the avidin-biotin-peroxidase complex (1:100, 30 min at RT) (ABC Vectastain Elite kit, Vector Labs). Antibody binding sites were revealed by incubating the sections in 0.25 mg/ml 3,3'-

diaminobenzidine (DAB) and 0.03 % H₂O₂ in PBS (10 min at RT). Negative controls were obtained by omitting the primary antibodies. Sections were mounted on gelatin-coated slides, dehydrated in a series of ethyl alcohols and xylene, dried and permanently coverslipped with Eukitt mounting medium (Kindler GmbH, Freiburg, Germany)

Cresyl violet staining

Three random sections of the SN from each of the series used for immunofluorescence of the MMP-9 knock out mice, and their matching WT mice, were stained with 1 % cresyl violet for 2 min. Following dehydration in a series of ethyl alcohol and xylene, sections were dried and permanently coverslipped with Eukitt mounting medium. Stereological quantification of the SN_{pc} neurons was performed as detailed in the next section.

Quantitative analysis

Immunohistochemistry. Number of TH⁺ neurons in the SN_{pc} and densitometric value of TH immunolabeling in the striatum, as well as number and area of GFAP⁺ and Iba1⁺ cells in both SN_{pc} and striatum of MMP-9 knock-out mice, revealed by the ABC-DAB method, were estimated on 3 representative sections *per* each mouse brain series. Sections were viewed with a Zeiss Axioplan 2 light microscope, connected to a digital camera, and one-two images of both areas were taken from each brain hemisphere using a 20X (SN_{pc}) and 1.25X (striatum) objectives. Density of immunopositive cells *per* area was expressed as the number of cells/mm². TH immunolabeling in the striatum was determined by the ImageJ software as optical density (O.D.) values and was considered as an index of the density of DA innervation. The area (μm²) occupied by microglia and astrocytes (including both cell bodies and processes), identified by specific labeling, was considered an index of glial cell activation and was expressed as both total and mean area occupied by immunopositive cells *per* photographic field. Mean cell area values were obtained by dividing the total area covered by immunopositive cells for their number. All data were generated by using the ImageJ software for image analysis. All quantifications were performed blindly.

Immunofluorescence. Three representative sections of the SN_{pc} and striatum of each control and MPTP-treated mice, and 2 from each control and parkinsonian macaque striatum, were chosen and 3 random images were captured from both sides of sections. Cells immunopositive for both MMP-9 and one of the cell markers used were counted only when the area of co-localization was detected in the majority of the 0.5 μ m-thick optical layers throughout the entire stack. The number of single and double immunolabeled cells was quantified on the best of the single 0.5 μ m-thick optical sections, and results were expressed as the number of immunopositive cells/mm². All quantifications were done blindly.

Statistical Analysis

Data were analyzed using either the one-way ANOVA test following the post-hoc Dunnett's test (adequate for multiple comparisons against a single reference group) or the two-tail Student's *t*-test (which compares two groups at a time). Differences were considered statistically significant for $p \leq 0.05$. Data were expressed as the mean \pm standard error of the mean (SEM). A Pearson coefficient was used for the correlation analysis and its significance was determined by using the critical values of the Pearson coefficient table. Differences were considered statistically significant for $p \leq 0.05$.

RESULTS

MMP-9 mRNA and protein levels are modulated in the nigro-striatal pathway by acute MPTP treatment in mice

mRNA levels for MMP-9 (gelatinase B) were investigated by real time RT-PCR. Based on previous studies (Annese et al., 2013), we explored a time window after the last MPTP injection that spanned the entire period of DA neuron degeneration and the partial recovery of those who escaped death, along with the rising and subsiding of neuroinflammatory events (Hirsch and Hunot 2009). MMP-9 mRNA was significantly and consistently induced, in both SN (Fig. 1a) and striatum (Fig. 1b), at different times after acute MPTP administration. mRNA levels were up-regulated (+1.8 folds, *SN*; + 2.2 folds, *striatum*) by 24 h after the last MPTP injection, remaining significantly higher than control in the following 48 h (+ 2.5 folds, *SN*) (Fig. 1a) and 1 w (+ 1.2 folds, *striatum*) (Fig. 1b).

MMP-9 protein levels were investigated by Western immunoblot in SN and striatum homogenates of control and parkinsonian mice, killed at the same post-treatment time as indicated above. The MMP-9 antibody revealed two bands of about 97 kDa (pro-MMP-9) and 92 kDa (active MMP-9) (Fig. 1c, *SN*; Fig. 1d, *striatum*). A human recombinant MMP-9, used as positive control and loaded on a separate lane in the same gels, appeared as a single band corresponding to the active MMP-9, and migrated slightly below its homologous in the mouse brain homogenates. Densitometric analysis of the immunopositive bands revealed that, similar to mRNA, protein levels of both pro- and active MMP-9 increased significantly by 24 h (Fig. 1c', *SN*) and 1 h (Fig. 1d', *striatum*) after MPTP administration, remaining higher than control throughout the post-treatment time considered. The apparent discrepancy in the post-injection times at which we observed the main changes in MMP-9 mRNA and protein levels, is a common event, especially for MMPs since these proteins are subjected to a prominent post-transcriptional control.

MMP-9 immunolocalization and quantitative analysis in control and MPTP-treated mice

The persistent and significant increase in MMP-9 protein levels in the SN and striatum of MPTP-treated mice involved both the inactive pro-enzyme and its active form (post-translationally activated). However, this analysis did not allow the identification of the type/s of cells expressing MMP-9 in control conditions. Moreover, this preliminary observation did not reveal the distribution changes after MPTP treatment and, less than that, whether and how active MMP-9 intervenes in: a) MPTP-induced DA neuron death in the SN and b) the neuroinflammatory process to which neurodegeneration associates. Therefore, we performed a confocal study, combined with quantitative analysis, for MMP-9 immunopositive (MMP-9⁺) cell localization in control and MPTP-treated mice. Brain sections were immunolabeled for MMP-9 alone or in combination with different cell type-specific markers: NeuN (neurons), TH (DA neurons), GSA (microglia) and GFAP (astrocytes).

Before this, we carried out both gelatin zymography (on SN and striatum tissue extracts) and *in situ* zymography (on brain sections), to verify the presence of MMP-9 activity in control and 72 h MPTP-treated mice (chosen as a representative post-injection time point). Gelatin zymography is a poorly sensitive and quite variable technique, and the signal we obtained from both SN and striatum was too low to be properly quantified (see also Lorenzl et al. 2004 on pools of entire midbrain extracts). *In situ* zymography, instead, showed that in both brain areas MPTP treatment elicited an increase in cellular and extracellular fluorescent signal, when compared to control (Fig. 2). Since the other gelatinase (gelatinase A, MMP-2), differently from MMP-9, is scarcely detectable at the protein level both before and after MPTP treatment (unpublished observation), we hypothesized that most of this labeling was generated by gelatinase B activation.

Confocal microscopy studies were performed on control and MPTP-treated mice killed 24 h, 48 h, 72 h and 2 w after the last toxin injection. Data will be presented subdivided by cell type (neuron, microglia, astrocytes).

MMP-9/NeuN/TH and MMP-9/NeuN co-localization in the SNpc and striatum of control and MPTP-treated mice.

To ascertain whether MMP-9 was synthesized by DA neurons in the SN_{pc} and whether this expression changed after MPTP administration, we performed a triple immunofluorescence, by combining anti-MMP-9 with both NeuN and TH immunolabeling. As shown in Fig. 3a, MMP-9 largely co-localized with NeuN and TH, in both control and Parkinsonian mouse brain sections, intensely decorating cell bodies and axons. Extracellular dots of immunoreactivity were also observed, likely representing transversally cut axons and/or secreted MMP-9. Quantitative analysis of the immunopositive cells showed that numerous NeuN⁺ cells expressed MMP-9 (Fig. 3a'). Among these, a large part of TH⁺ neurons were also MMP-9⁺ (Fig. 3a''), and the majority of NeuN⁺ neurons were DA (TH⁺) (Fig. 3a''), in both control and Parkinsonian mice. As expected, MPTP-treatment determined a significant decrease in MMP-9⁺ cells within the following 24 h (Fig. 3a'); this coincided with a significant decrease in the total number of neurons (NeuN⁺ in Fig. 3a') and TH⁺ neurons (Fig. 3a''), both alone and in co-localization with MMP-9, clearly noticeable also in the confocal images (Fig. 3a). The number of all immunopositive cells (MMP-9⁺, NeuN⁺, NeuN⁺/MMP-9⁺, TH⁺ and TH⁺/MMP-9⁺) partially, but significantly, recovered 2 w after MPTP administration (Fig. 3a', 3a''). This pattern was further verified in the second part of this work (conducted on MMP-9 KO mice) and confirmed by a parallel study, in which TH⁺ neurons, revealed by the immuno-enzymatic method of the HRP-DAB, were counted in SN_{pc} sections, serial to those used in this study (Annese et al. 2013). Changes in TH protein levels in the SN were also quantified by densitometric analysis of Western immunoblot (Fig. 4a, a') and results were in accord to what was shown by immunohistochemistry.

From this quantitative study, it also emerged that the number of non-DA neurons (NeuN⁺/TH⁻) remained stable after MPTP treatment (Fig. 3a''), indicating that the toxin does not affect this type of neurons in the SN_{pc}. Moreover, the number of non-DA neurons expressing MMP-9 (NeuN⁺/MMP-9⁺/TH⁻) increased slightly, but significantly, 72 h after the last MPTP injection (Fig. 3a''), suggesting that factors, possibly released by dying and/or suffering DA

neurons, as well as by other types of cells, may trigger MMP-9 expression in the surrounding neurons.

Similar to the SNpc, MMP-9 immunolabeling in the striatum largely co-localized with NeuN, although not all neurons were MMP-9⁺ and not all MMP-9⁺-cells were neurons (Fig. 3b). Seventy-two hours after the last MPTP injection, a clear increase in MMP-9 immunolabeling was observed. Large part of the staining was visible outside the cell bodies, being present not only in the extracellular space, but also within the thin processes of non-neuronal cells (see ahead in Results), and into transversally-cut axons crossing the striatum (Fig. 3b). Quantitative analysis showed that the number of MMP-9⁺ cells increased significantly, with respect to control, by 48 h after MPTP injection, remaining higher than control up to 2 w after (Fig. 3b'). Contrarily, the number of neurons, both positive (NeuN⁺/MMP-9⁺) and negative (NeuN⁺) for MMP-9, did not change after treatment, suggesting that the increase in MMP-9⁺ cells may depend on activated and/or newly migrated non-neuronal cells.

Concomitant to confocal analysis, we evaluated TH levels in the striatum of control and MPTP-treated mice by Western immunoblot. Figure 4b,b' shows that TH levels significantly decreased with respect to control, 24 h and 48 h after MPTP treatment, being recovered in the following time points but remaining below the control values. This is in agreement with the results obtained by densitometric evaluation of TH immunolabeling performed on striatum sections adjacent to those utilized in this study (Annese et al. 2013), as well as on sections from WT and MMP-9 KO mice (see ahead in Results).

MMP-9/GSA co-localization in the SNpc and striatum of control and MPTP-treated mice.

Microglia, the brain immune resident cells, are main modulators of neuroinflammation. As reported in the Introduction, in both PD patients and MPTP animal models of Parkinsonism, microglia shift from “surveillant” to “active”, modify their morphology, and acquire migratory and phagocyte capabilities, according to a well-described step-to-step response (Streit et al. 1999). Here, we investigated whether MMP-9 was expressed by microglia and whether this expression was

modulated by acute MPTP-treatment. For this purpose, we combined MMP-9 immunolabeling with GSA staining, a classical marker for microglia, widely used in the literature to identify both resting and activated microglia (Streit and Kretuzberg 1987; Pott Godoy et al. 2008). The choice of GSA was dictated by a technical impediment when combining MMP-9 and microglia immunolabeling protocols by using the classical Iba-1 or F4-80 antibodies. MPTP-induced microgliosis was, however, subsequently confirmed and quantified in the following experiments conducted on WT and MMP-9 KO mice (see ahead in Results). For the MMP-9/GSA analysis, we used a classical fluorescent microscope, as the rodamine labeling was rapidly fading under the confocal beam. In both control SNpc and striatum, GSA staining was scanty, mainly associated with blood vessels and small cell processes (Fig. 5a, SNpc). The number of GSA⁺ cells significantly and progressively increased from 24 h to 72 h after MPTP-treatment (Fig. 5a; Fig. 5a', *quantitative analysis*) and then significantly decreased (compared to the 72 h time point) after 2 w, although remained higher than control. In control mice, coexistence of GSA and MMP-9 (GSA⁺/MMP-9⁺) was rarely observed in both SNpc (Fig. 5a', *quantitative analysis*) and striatum (Fig. 5c, *quantitative analysis*). By 24 h after MPTP treatment, the number of GSA⁺/MMP-9⁺ cells significantly increased in both areas, with respect to control (SNpc: Fig. 5a', *quantitative analysis*; striatum: Fig. 5c, *quantitative analysis*), overlapping with the period of major loss of TH⁺ neurons in the SNpc and decrease in TH⁺ fibers in the striatum. Differently from neurons, MMP-9 immunolabeling in GSA⁺ cells appeared in small discrete dots, possibly representing points of accumulation/release. Two weeks later, while in the SNpc the number of GSA⁺/MMP-9⁺ cells returned to control levels, concomitantly with the partial recovery of TH⁺ neurons, in the striatum it remained significantly higher than control.

MMP-9/GFAP co-localization in the SNpc and striatum of control and MPTP-injected mice.

Since astrogliosis commonly follows microglia activation in neuroinflammatory processes, we evaluated MMP-9 expression in astrocytes by co-localizing it with the cell-specific marker GFAP. Confocal analysis showed that, after MPTP treatment, both SNpc (Fig. 5b) and striatum underwent

prominent astrogliosis. The number of GFAP⁺ cells increased significantly after 24 h (Fig. 5b', SNpc; Fig. 5d, striatum), remaining higher than control up to 2 w. The number of astrocytes expressing MMP-9 (GFAP⁺/MMP-9⁺) increased with the same time course than the number of GFAP⁺ cells. As for microglia, the number of double immunolabeled cells (Fig. 5b) represented only a small percentage of the whole MMP-9⁺ cell population.

A summary of the changes in the percentage of the different MMP-9⁺ cell types, emerged from the confocal and quantitative analyses, is shown in the pie charts of Fig. 6. In control conditions, MMP-9 is mainly expressed by neurons, in both SNpc and striatum. The number of immunopositive glial cells increases significantly after MPTP treatment, concomitantly with microgliosis and astrogliosis, and remains higher than control up to 2 w. Sector indicated as “others” comprehend a category of mixed cells, not identified in this study. A large part of these cells is certainly represented by oligodendrocytes (unpublished observation), which undergo massive oligodendroglia (Annese et al. 2013). The rest could be blood-born immune cells crossing the damaged blood brain barrier, attracted by the inflammatory process; however, their identity needs to be properly investigated.

MMP-9 immunolocalization and quantitative analysis in control and parkinsonian macaques

The mouse model of Parkinsonism has the advantage of a fast analysis of the cellular and molecular processes related to the nigro-striatal pathway degeneration. On the other hand, the use of the chronic macaque model of MPTP administration is extremely important for a better understanding of the role of inflammatory processes in the long-term disease progression, more similar to what happens in humans. We had the opportunity to use sections of the striatum (both *caudate* and *putamen*) of previously studied macaques (Barcia et al. 2004, 2011). These samples were already well characterized for the loss of DA neurons and axons, as well as for microglia activation. Here, we evaluated MMP-9 expression, alone and in combination with some of the specific markers used above (NeuN, GFAP), in the striatum of both control and parkinsonian macaques (2 years after

MPTP-induced stable Parkinsonism). Similar to mice, MMP-9 immunolabeling co-localized with the neuronal marker NeuN (Fig. 7a), although numerous MMP-9⁻ neurons were also present. MPTP treatment induced a clear up-regulation in MMP-9 immunolabeling in both areas with respect to control (Fig. 7a). Quantitative analysis confirmed a significant increase in both MMP-9⁺ cells and NeuN⁺/MMP-9⁺ labeled neurons (Fig. 7a'). The total number of NeuN⁺ neurons, instead, remained comparable to control, suggesting that striatal neurons, previously immunonegative, were induced to express MMP-9 in parkinsonian primates. Numerous MMP-9⁺/NeuN⁻ cells, with an apparent glial morphology and scarcely present in control monkeys, were also observed (Fig. 7a).

GFAP immunolabeling showed a dramatic and persistent astrogliosis in the striatum of MPTP-treated monkeys when compared to control animals (Fig. 7b). Astrocyte activation was characterized by an increase in cell size, as well as in the number and length of cell processes (Fig. 7b). GFAP/MMP-9 co-immunolabeling (MMP-9⁺/GFAP⁺) showed that astroglia represented only a small percentage of MMP-9⁺ cells, in both control and parkinsonian monkeys. However, after MPTP treatment, the number of MMP-9⁺/GFAP⁺ cells increased significantly with respect to control (Fig. 7b'). For the same technical reasons described for mice, we were unable to combine MMP-9 staining with classical markers of microglial cells.

Evaluation of nigro-striatal pathway degeneration and progression of neuroinflammation in MMP-9 KO and wild-type mice

Based on the results obtained so far, the main question remaining was related to whether MMP-9 could play a primary role in MPTP-induced neuroinflammation and, as a consequence, on SNpc DA neuron death. To unravel this question, we acutely treated MMP-9 KO mice and their matching WT with MPTP. Animals were killed 72 h and 2 w after MPTP administration, chosen as the most representative dates in the neuroinflammatory response of the nigro-striatal pathway. We performed HRP-DAB immunohistochemistry for: a) TH, to quantify DA neuron death in the SNpc and the

decrease in DA innervation in the striatum; b) Iba-1, to evaluate number and size of microglia; c) GFAP, to evaluate number and size of astrocytes.

Quantification of TH-immunoreactivity in the SNpc and striatum of wild-type and MMP-9 KO mice after MPTP treatment.

In both WT and MMP-9 KO mice, TH immunolabeling in the SN revealed the characteristic distribution of DA neurons in the *pars compacta* (Fig. 8a). However, the number of DA neurons (TH⁺) in untreated MMP-9 KO mice, was lower than in the WT, although this difference was not significant ($p = 0.18$). Due to this initial difference, to clearly evaluate changes in DA neuron number after MPTP treatment, we expressed this value as the percentage compared to control. MPTP treatment elicited significant loss of TH⁺ neurons in the SNpc of both genotypes 72 h after the last MPTP injection (Fig. 8a; Fig. 8b, *quantitative analysis*). However, in MMP-9 KO mice, this reduction was significantly lower with respect to control, with 54 % of TH⁺ neurons left in the wild type mice *versus* 82 % in MMP-9 KO mice (Fig. 8b). As expected, 2 w after MPTP treatment, the percentage of TH⁺ neurons increased in both genotypes (Fig. 8a; Fig. 8b, *quantitative analysis*), being in MMP-9 KO mice not significantly different than in the control mice (Fig. 8b). To further investigate this point, midbrain sections of control and MPTP-treated mice were stained with cresyl violet and the total number of neurons counted. The graph in Fig. 8c shows a significant neuronal loss 72 h after MPTP injection, which does not recover after 2 w. Moreover, the number of neurons in MPTP-treated KO mice is always significantly higher than that in the WT. This result definitely demonstrate that, after MPTP treatment, not all SNpc neurons die, but a number of affected neurons just stop synthesizing and transporting TH along the axons, being able to recover from toxic treatment.

In the striatum, TH immunolabeling (evaluated as O.D. of gray scale units) was lower, although not significantly ($p = 0.44$), in MMP-9 KO mice with respect to WT (Fig. 8d; Fig. 8e, *densitometric analysis*), reasonably due to the presence of a fewer number of DA neurons in the SNpc of control mice. MPTP administration elicited a significant decrease (72 h) and successive

recovery (2 w *versus* 72 h) in TH immunolabeling, although values remained lower than controls (Fig. 8d; Fig. 8e, *densitometric analysis*). Differently from the SNpc, no significant differences were observed in the striatum between WT and MMP-9 KO mice at both 72 h and 2 w after MPTP treatment, although the recovery of TH immunolabeling in the KO mice was more significant ($p < 0.05$, when evaluated by the Student's *t*-test) than in the WT. Once more, these data suggest that lack of MMP-9 protects DA neurons from death, reflected also in a higher degree of striatal DA reinnervation.

Quantification of Iba-1-immunopositive (Iba-1⁺) cells in the SNpc and striatum of wild-type and MMP-9 KO mice after MPTP treatment.

We performed immunolabeling on brain sections, adjacent to those immunoreacted for TH, with an antibody directed against Iba-1, a microglia cell-specific protein, which labels both resting and active microglia. Fig. 9a shows Iba-1 immunoreactivity in the SN of control and MPTP-treated mice. Differences in the overall intensity of immunolabeling between experimental groups can be appreciated, as well as the appearance of large and intensely labeled Iba-1⁺ cells 72 h after MPTP treatment in both WT and MMP-9 KO mice. Details of microglial cells in WT (Fig. 9a¹, *control*; Fig. 9a², *72 h MPTP*) and MMP-9-KO (Fig. 9a³, *control*; Fig. 9a⁴, *72 h MPTP*) mice clearly show an increase in cell size and in the amount of processes after MPTP treatment with respect to untreated controls, in both genotypes. However, changes in WT mice are more pronounced than in MMP-9 KO mice. These differences were confirmed by quantitative analysis, in which we evaluated mean cell number/area, mean area/cell and total area occupied by all Iba1⁺ cells. The number of microglial cells increased significantly 72 h after MPTP treatment, and began to decline by 2 w compared to the 72 h time point, although remaining higher than control (Fig. 9b). We did not observe differences in cell numbers between the two genotypes, in both control and MPTP-treated mice, meaning that the absence of MMP-9 does not affect microglia cell generation, division and recruitment to the site of damage. Both mean cell area (Fig. 9c) and total area/field occupied by Iba1⁺ cells (not shown) changed according to cell number. However, 72 h after treatment, when

microglia activation is at its maximum, these values were significantly lower in MMP-9 KO mice with respect to WT mice.

In the striatum, results were comparable to those in the *SNpc*. Figure 9d is representative of Iba-1 immunolabeling in the different experimental groups. Insets into the figures highlight the morphological characteristics of individual cells, in which differences in cell size between WT and MMP-9 KO mice after MPTP treatment can be appreciated. Statistical analyses relative to Iba-1⁺ cell number (Fig. 9e), mean cell area (Fig. 9f), and total area/field occupied by Iba1⁺ cells (not shown) are in accord to the statistics in the *SNpc*. As a notable exception, 2 w after MPTP treatment, mean cell size remains higher in WT animals compared to untreated controls, suggesting a prolongation of the inflammatory reaction with respect to what happens in the SN.

Quantification of GFAP-immunopositive (GFAP⁺) cells in the SNpc and striatum of wild-type and MMP-9 KO mice after MPTP treatment.

Figure 10a shows GFAP immunolabeling in sections of the SN from control and MPTP-treated WT and MMP-9 KO mice. Intensity and distribution of the immunostaining increased 72 h after MPTP injection with respect to control, decreasing again after 2 w. Astrocyte morphological changes after MPTP treatment in WT (Fig. 10a¹, *control*; Fig. 10a², *72 h MPTP*) and MMP-9-KO (Fig. 10a³, *control*; Fig. 10a⁴, *72 h MPTP*) mice are shown. Quantitative analysis of the changes in GFAP⁺ cell number (Fig. 10b), mean cell size (Fig. 10c), and total area/photographic field occupied by GFAP⁺ cells (not shown) was fairly similar to what was previously described for microglia: i.e. all parameters increased 72 h after MPTP treatment and began to decline within 2 w. Similar to microglia, 72 h after MPTP administration, the absence of active MMP-9 did not produce differences between the two genotypes in terms of astrocyte cell numbers (Fig. 10b), but only in cell size (Fig. 10c).

In the striatum, results were comparable to those in the *SNpc*. Figure 10d shows GFAP immunolabeling in control WT and MMP-9 KO mice and the changes after MPTP treatment

(details of single astrocytes for each experimental group are shown in the inset of figures). Quantitative analyses are reported in Fig. 10e (GFAP⁺ cell number) and Fig. 10f (mean cell area).

Data collected from the experiments on WT and MMP-9 KO mice were compared to each other in a correlation study. A significant inverse correlation between cell number and size (mean and total area) of both Iba-1⁺ and GFAP⁺ cells and a decrease in TH⁺ cell number and TH⁺ fibers in the *SNpc* and striatum respectively, were observed (Fig. 11).

DISCUSSION

Neuroinflammation is a feature of PD common to several brain pathologies. Its cellular and molecular aspects have, therefore, become a major field of investigation as a unifying ground on the causative and/or aggravating element of neurodegenerative diseases. Animal models of Parkinsonism, as those adopted in this study, allow the identification of the temporal and cellular basis of neuroinflammation, its correlation with the primary degeneration of DA nigro-striatal pathway and the molecular signals involved.

After MPTP intoxication, microglia is early recruited, followed by T-cell infiltration and astrogliosis when neuronal loss has already progressed (Hirsch and Hunot 2009). Perpetuation of microgliosis can, therefore, be a crucial non-turning point for neuron degeneration. After a harmful event, reactive microglia is involved in scavenging neuronal debris; however an adverse role emerges when pro-inflammatory cytokines (i.e. $\text{INT-}\gamma$; $\text{TNF-}\alpha$) perpetuate inflammation, favoring neurodegeneration (Barcia et al. 2005, 2011; Pott Godoy et al. 2008). In this study, MPTP-treated mice develop a prominent but transient inflammation, which coincides with DA neuron and fiber degeneration; successive remission of this inflammation correlates with functional recovery of surviving neurons. By combining TH immunohistochemistry and cresyl violet staining, we confirmed that part of the DA neurons in the lesioned *SNpc* may be only temporarily affected, remaining functionally silent for a short time and with great potentiality to survive intoxication and to partially reinnervate the striatum, as previously reported in both MPTP-treated mice and monkeys (Bezard et al. 2000; Mounayar et al. 2007). Although the observations in mice are different than the irreversible degeneration that MPTP provokes in humans (Langston et al. 1983) and monkeys (Barcia et al. 2004), these results pose a new ground for studies aimed at uncovering molecular mechanisms promoting rescue of affected neurons and re-establishing nigro-striatal connections.

The major point of this study was to identify factors responsible for the perpetuation of glia proliferation and/or activation, which shifts a beneficial response, intended to maintain brain homeostasis, into a deadly chronic state. A role could be played by MMPs, involved in several CNS injuries and diseases, but at the same time promoters of neuro-reparative and physiological processes (Yong 2005; Zhang et al. 2010; De Stefano et al. 2012). MMPs detrimental role relies on the unbalance of the delicate equilibrium between activation and inhibition; therefore, re-establishment of this equilibrium could be a therapeutic strategy aimed at modulating neuroinflammation.

Related to Parkinsonism, *in vitro* studies have demonstrated intracellular activation of MMP-3 after neuronal stress, with consequent induction of apoptotic-signaling cascades (Choi et al. 2008; Kim et al. 2010). MMP-3 released by dying neurons activates microglia, further contributing to neurodegeneration (Kim et al. 2007) along with MMP-9 (Woo et al. 2008). Altered gelatinase expression in the SN of post-mortem brains of PD patients was first reported by Lorenzl et al. (2002), according to whom no alteration in MMP-9 protein and activity levels were observed compared to age-matched controls. Later on, the same authors reported an increase in MMP-9 mRNA, protein, and activity levels in the SN and striatum of pools of MPTP-treated mice (Lorenzl et al. 2004), although these data were not detailed in terms of post-injection times, and lacked a proper quantitative/qualitative evaluation of the type/s of cells in which MMP-9 expression was modulated. According to our data, MMP-9 indeed turns out to be highly expressed and modulated in mouse SN_{pc} and striatum from the very first stages of MPTP-induced neuroinflammation, and throughout the 2 w period of observation. Qualitative and quantitative data, obtained by co-immunolabeling MMP-9 with different cell-specific markers, show significant enhancement of MMP-9 expression in reactive microglia and astrocytes recruited in SN_{pc} and striatum. This is in accord to the literature, where it is reported that neurons, microglia and astrocytes synthesize both gelatinases (MMP-2 and MMP-9), although MMP-9 is the only highly modulated under experimental conditions (Yong 2005; Wilczynski et al. 2008; Candelario-Jalil et al. 2009; Walker

and Rosenberg 2010). In MPTP-injected mice, neuroinflammation is transient and starts decreasing within 2 w after the treatment, when the number of MMP-9⁺ microglia and astrocytes in the nigro-striatal pathway declines to control levels. This overlaps the partial recovery of TH protein levels and TH⁺ neurons and fibers (Annese et al. 2013; this study), suggesting that glial MMP-9 is a major player in the ignition of neuroinflammation. Specifically, based on the results obtained in KO mice, MMP-9 appears to be important for glia “activation”, but not proliferation. In fact, 72 h after MPTP treatment, while the number of microglia and astrocytes in both SNpc and striatum of WT and MMP-9 KO mice are similar, mean cell size and the total area that reactive glia occupies *per* section are significantly higher in WT mice. This difference disappears after 2 w, when inflammation is subsiding. In the striatum, both the number of MMP-9⁺ glial cells and TH protein levels decline slower than in the SNpc, possibly related to its complex circuitry. Striatal response to MPTP is prompt, as the toxin first affects SNpc neuron activity and viability (Herkenham et al. 1991), with consequent striatal neuronal denervation and retrograde reaction of cortical neurons, which also project to the striatum, exacerbating and prolonging the inflammatory process.

Data on MMP-9 KO mice indicate that inflammatory glia hampers neuron survival, as a reduction in reactive glia with respect to WT correlates with a higher number of TH⁺ neurons (functional DA neurons) and cresyl violet-stained neurons (effective number of neurons) in the SNpc, at both 72 h and 2 w post-treatment. We do not exclude that MMP-9, early released by affected DA neurons, may contribute to neuronal death by disrupting cell-cell and cell-ECM linkage (Kim et al. 2009).

A role of MMP-9 in the exacerbation of inflammation is also suggested by the results on parkinsonian macaques, where MPTP-induced long-lasting neuroinflammation correlates with progressive degeneration of nigro-striatal circuitry. The numbers of MMP-9⁺ striatal neurons and astrocytes increase when compared to control, suggesting that molecular signals released by "denervated" neurons and axons support the inflammatory environment. MMP-9 could be a good candidate, as can favor migration of glial cells by cleaving/modifying cell surface receptors,

activating chemotactic factors and pro-inflammatory chemokines (IL-1 β , TNF- α) (Kawasaki et al. 2008), and degrading ECM proteins. On the other hand, TNF- α and IL-1 β induce a prominent release of MMP-9 by glial cells (Kauppinen and Swanson 2005), which in turn amplify their reactive state (Sbai et al. 2010), further modifying cell size and enhancing amoeboid movements (Fig. 12).

MMP activity can switch from harmful to reparative, allowing axon re-growth, remyelination and re-establishment of connectivity (Yong 2005; Agrawal et al. 2008, Huntley 2012; De Stefano et al. 2012). In particular, oligodendrocyte-derived MMP-9 supports oligodendrogliosis and myelin restoration (Uhm et al. 1998; Oh et al. 1999; Larsen et al. 2003). We previously demonstrated that MPTP treatment of both mice and monkeys induces a prominent oligodendrogliosis concomitant to the inflammatory process here described (Annese et al. 2013). In this study, a number of cells classified as “others”, among which there are oligodendrocytes (unpublished observation), express MMP-9, both before and after MPTP treatment. Therefore, we hypothesize that, in parkinsonian mice, persistent expression of active MMP-9 may be implicated in late reparative processes by: mediating oligodendrogliosis, which implies myelin digestion and cell remodeling; favoring elongation and sprouting of regenerating axon once released by growth cones, by remodeling ECM proteins; supporting formation of new myelin sheaths and oligodendrocyte-axon connections (Larsen et al. 2003, 2006). These events have been summarized in the cartoon depicted in Fig. 12, which takes into account both previous (Annese et al. 2013) and present results for a more comprehensive picture.

Results obtained in MPTP-treated macaques differ, but do not contradict, those described in mice. Two years after establishment of stable Parkinsonism, in the monkey striatum both inflammation (this study; Barcia et al. 2004, 2011) and oligodendrogliosis (Annese et al. 2013) are significantly higher than in control animals. Differences inter species (macaque *vs* mouse) and/or MPTP administration modality (chronic *vs* acute) determine pathological traits more similar in the macaque to human PD. Therefore, neuronal damage initiates a cascade of glia-derived and auto-

perpetuating inflammatory signals, which favor progressive DA neuron loss (Brochard et al. 2009), and promote formation of a glial scar. This would impose a barrier to axon regeneration (Rolls 2009) and create a hostile environment, in which oligodendrocyte activity becomes ineffective (Goldschmidt et al. 2009).

In conclusion, MMP-9 could be a possible therapeutic target for the treatment of acute neuroinflammation in Parkinsonism. However, MMP roles in physiological and reparative processes, and the perfect timing at which beneficial effects can revert into detrimental, complicate the efforts of treatment with MMP inhibitors. Therefore, models reproducing developmental stages of the disease are useful to clarify time and place of MMP activation in order to devise therapeutic strategies.

Acknowledgments: The authors wish to thank Prof. P. Paggi for her valuable comments and stimulating discussions. This work was supported by grants from: MIUR (*Ministero dell'Università e della Ricerca Scientifica*, Ricerche Universitarie 2011), ASI (*Agenzia Spaziale Italiana*) and Fundación Séneca (14902/IV10/10) to MEDS and by grants from: the Spanish Ministry of Science (SAF07-062262, FIS PI10-02827), Fundación Séneca (FS/15329/PI/10), UJI (13I004.01/1) and CIBERNED (*Centro de Investigación Biomédica en Red sobre Enfermedades Neurodegenerativas*) to MTH.

REFERENCES

- Agrawal SM, Lau L, Yong VW (2008) MMPs in the central nervous system: where the good guys go bad. *Semin Cell Dev Biol* 19:42-51
- Annese V, Barcia C, Ros-Bernal F, Gómez A, Ros CM, De Pablos V, Fernández-Villalba E, De Stefano ME, Herrero MT (2013) Evidence of oligodendrogliosis in 1-methyl-4-phenyl-1,2,3,6-tetrahydropyridine (MPTP)-induced Parkinsonism. *Neuropathol Appl Neurobiol* 39:132–143
- Barcia C, Bautista V, Sánchez-Bahillo A, Fernández-Villalba E, Navarro-Ruis JM, Barreiro AF, Poza Y, Poza M, Herrero MT (2003) Circadian determinations of cortisol, prolactin and melatonin in chronic methyl-phenyl-tetrahydropyridine-treated monkeys. *Neuroendocrinol* 78:118-128
- Barcia C, Sánchez-Bahillo A, Fernández-Villalba E, Bautista V, Poza Y, Poza M, Fernández-Barreiro A, Hirsch EC, Herrero MT (2004) Evidence of active microglia in substantia nigra pars compacta of parkinsonian monkeys 1 year after MPTP exposure. *Glia* 46:402-409
- Barcia C, de Pablos V, Bautista-Hernández V, Sánchez-Bahillo A, Bernal I, Fernández-Villalba E, Martín J, Bañón R, Fernández-Barreiro A, Herrero MT (2005) Increased plasma levels of TNF-alpha but not of IL1-beta in MPTP-treated monkeys one year after the MPTP administration. *Parkinsonism Relat Disord.* 11:435-439
- Barcia C, Sanderson NSR, Barrett RJ, Wawrowsky K, Kroeger KM, Puntell M, Liu C, Castro MG, Lowenstein PR (2008) T cells' immunological synapses induce polarization of brain astrocytes *in vivo* and *in vitro*: a novel astrocyte response mechanism to cellular injury. *Plos ONE* 3: e2977
- Barcia C, Ros CM, Annese V, Gómez A, Ros-Bernal F, Aguado-Yera D, Martínez-Pagán ME, de Pablos V, Fernandez-Villalba E, Herrero MT (2011) IFN- γ signaling, with the synergistic contribution of TNF- α , mediates cell specific microglial and astroglial activation in experimental models of Parkinson's disease. *Cell Death Dis* 2:e142

- Barnum CJ, Tansey MG (2010) Modeling neuroinflammatory pathogenesis of Parkinson's disease. *Prog Brain Res* 184:113-132
- Bezard E, Dovero S, Imbert C, Boraud T, Gross CE (2000) Spontaneous long-term compensatory dopaminergic sprouting in MPTP-treated mice. *Synapse* 38:363-368
- Braak H, Rüb U, Gai WP, Del Tredici K (2003) Idiopathic Parkinson's disease: possible routes by which vulnerable neuronal types may be subject to neuroinvasion by an unknown pathogen. *J Neural Transm* 110:517-536
- Braak H, Del Tredici K, Rüb U, de Vos RA, Jansen Steur N, Braak E (2006) Staging of brain pathology related to sporadic Parkinson's disease. *Neurobiol Aging* 24:197-211
- Braak H, Sastre M, Del Tredici K (2007) Development of α -synuclein immunoreactive astrocytes in the forebrain parallels stages of intraneuronal pathology in sporadic Parkinson's disease. *Acta Neuropathol* 114:231-241
- Brochard V, Combadière B, Prigent A, Laouar Y, Perrin A, Beray-Berthat V, Bonduelle O, Alvarez-Fischer D, Callebert J, Launay JM, Duyckaerts C, Flavell RA, Hirsch EC, Hunot S (2009) Infiltration of CD4⁺ lymphocytes into the brain contributes to neurodegeneration in a mouse model of Parkinson disease. *J Clin Invest* 119:182-192
- Candelario-Jalil E, Yang Y, Rosenberg GA (2009) Diverse roles of matrix metalloproteinases and tissue inhibitors of metalloproteinases in neuroinflammation and cerebral ischemia. *Neuroscience* 158:983-994
- Choi DH, Kim EM, Son HJ, Joh TH, Kim D, Beal MF, Hwang O (2008) A novel intracellular role of matrix metalloproteinase-3 during apoptosis of dopaminergic cells. *J Neurochem* 106:405-415

- Del Signore A, De Sanctis V, Di Mauro E, Negri R, Perrone-Capano C, Paggi P (2006) Gene expression pathways induced by axotomy and decentralization of rat superior cervical ganglion neurons. *Eur J Neurosci* 23:65-74
- De Stefano ME, Annese V, Barcia C, Ros Bernal F, Fernandez-Villalba E, Herrero MT (2012) Neuroinflammation in Parkinson's disease: a role for matrix metalloproteinases? In: Gemma C (ed) *Neuroinflammation: Pathogenesis, Mechanisms and Management*. Nova Science Publishers, Inc, Hapauge, NY
- Gerard M, Debyser Z, Desender L, Kahle PJ, Baert J, Baekelandt V, Engelborghs Y (2006) The aggregation of alpha-synuclein is stimulated by FK506 binding proteins as shown by fluorescence correlation spectroscopy. *FASEB J* 20:524-526
- Goldschmidt T, Antel J, König FB, Brück W, Kuhlmann T (2009) Remyelination capacity of the MS brain decreases with disease chronicity. *Neurology* 72:1914-1921
- Herkenham M, Little MD, Bankiewicz K, Yang SC, Markey SP, Johannessen JN (1991) Selective retention of MPP⁺ within the monoaminergic systems of the primate brain following MPTP administration: an in vivo autoradiographic study. *Neuroscience* 40:133-58
- Herrero MT, Hirsch EC, Javoy-Agid F, Obeso JA, Agid Y (1993) Differential vulnerability to 1-methyl-4-phenyl-1,2,3,6-tetrahydropyridine of dopaminergic and cholinergic neurons in the monkey mesopontine tegmentum. *Brain Res* 624:281-285
- Hirsch EC, Hunot S, Damier P, Faucheux B (1998) Glial cells and inflammation in Parkinson's disease: a role in neurodegeneration? *Ann Neurol* 44:S115-S120
- Hirsch EC, Hunot S (2009) Neuroinflammation in Parkinson's disease: a target for neuroprotection? *Lancet Neurol* 8:382-397

Houlden H, Singleton AB (2012) The genetics and neuropathology of Parkinson's disease. *Acta Neuropathol* 124:325-338

Hunot S, Boissiere F, Faucheux B, Brugg B, Mouatt-Prigent A, Agid Y (1996) Nitric oxide synthase and neuronal vulnerability in Parkinson's disease. *Neuroscience* 72:355-363

Huntley GW (2012) Synaptic circuit remodelling by matrix metalloproteinases in health and disease. *Nat Rev Neurosci* 13:743-757

Jackson-Lewis V, Jakowec M, Burke RE, Przedborski S. (1995) Time course and morphology of dopaminergic neuronal death caused by the neurotoxin 1-methyl-4-phenyl-1,2,3,6-tetrahydropyridine. *Neurodegeneration* 4:257-269

Kauppinen TM, Swanson RA (2005) Poly(ADP-ribose) polymerase-1 promotes microglial activation, proliferation, and matrix metalloproteinase-9-mediated neuron death. *J Immunol* 174:2288-96

Kawasaki Y, Xu ZZ, Wang X, Park JY, Zhuang ZY, Tan PH, Gao YJ, Roy K, Corfas G, Lo EH, Ji RR (2008) Distinct roles of matrix metalloproteases in the early- and late-phase development of neuropathic pain. *Nat Med* 14:331-336

Kim E-M, Shin E-J, Choi JH, Son HJ, Park I-S, Joh TH, Hwang O (2010) Matrix metalloproteinase-3 is increased and participates in neuronal apoptotic signaling downstream of caspase-12 during endoplasmic reticulum stress. *J Biol Chem* 285:16444-16452

Kim GW, Kim HJ, Cho KJ, Kim HW, Cho YJ, Lee BI (2009) The role of MMP-9 in integrin-mediated hippocampal cell death after pilocarpine-induced status epilepticus. *Neurobiol Dis* 36:169-80

Kim SK, Kang SW, Kim DH, Yun DH, Chung JH, Ban JY (2011) Matrix metalloproteinase-3 gene

polymorphisms are associated with ischemic stroke. *J Interferon Cytokine Res* 32:81-86

Kim YS, Kim SS, Choi DH, Hwang O, Shin DH, Chun HS, Beal MF, Joh TH (2005) Matrix metalloproteinase-3: a novel signaling proteinase from apoptotic neuronal cells that activates microglia. *J Neurosci* 25:3701-3711

Kim YS, Choi DH, Block ML, Lorenzl S, Yang L, Kim YJ, Sugama S, Cho BP, Hwang O, Browne SE, Kim SY, Hong J-S, Beal MF, Joh TH (2007) A pivotal role of matrix metalloproteinase-3 activity in dopaminergic neuronal degeneration via microglial activation. *FASEB J* 21:179-180

L'Episcopo F, Tirolo C, Caniglia S, Testa N, Serra PA, Impagnatiello F, Morale MC, Marchetti B (2010) Combining nitric oxide release with anti-inflammatory activity preserves nigrostriatal dopaminergic innervation and prevents motor impairment in a 1-methyl-4-phenyl-1,2,3,6-tetrahydropyridine model of Parkinson's disease. *J Neuroinflammation* 7:83

Langston JW, Ballard P, Tetrud JW, Irwin I (1983) Chronic Parkinsonism in humans due to a product of meperidine-analog synthesis. *Science* 219:979-980

Larsen PH, Wells JE, Stallcup WB, Opdenakker G, Yong VW (2003) Matrix metalloproteinase-9 facilitates remyelination in part by processing the inhibitory NG2 proteoglycan. *J Neurosci* 23:11127-11135

Larsen PH, DaSilva AG, Conant K, Yong VW (2006) Myelin formation during development of the CNS is delayed in matrix metalloproteinase-9 and -12 null mice. *J Neurosci* 26:2207-2214

Leonardo CC, Pennypacker KR (2009) Neuroinflammation and MMPs: potential therapeutic targets in neonatal hypoxic-ischemic injury. *J Neuroinflammation* 6:13

Livak KJ, Schmittgen TD (2001) Analysis of relative gene expression data using real-time quantitative PCR and the $2^{-\Delta\Delta C(T)}$ Methods 25:402-408

Lorenzl S, Albers DS, Narr S, Chirichigno J, Beal MF (2002) Expression of MMP-2, MMP-9, and MMP-1 and their endogenous counterregulators TIMP-1 and TIMP-2 in postmortem brain tissue of Parkinson's disease. *Exp Neurol* 178:13-20

Lorenzl S, Calingasan N, Yang L, Albers DS, Shugama S, Gregorio J, Krell HW, Chirichigno J, Joh T, Beal MF (2004) Matrix metalloproteinase-9 is elevated in 1-methyl-4-phenyl-1,2,3,6-tetrahydropyridine-induced parkinsonism in mice. *Neuromolecular Med* 5:119-132

McGeer PL, Itagaki S, Boyes BE, McGeer EG (1988) Reactive microglia are positive for HLA-DR in the substantia nigra of Parkinson's and Alzheimer's disease brains. *Neurology* 38:1285-1291

Mounayar S, Boulet S, Tandé D, Jan C, Pessiglione M, Hirsch EC, Féger J, Savasta M, François C, Tremblay L (2007) A new model to study compensatory mechanisms in MPTP-treated monkeys exhibiting recovery. *Brain* 130:2898-2914

Nagatsu T, Mogi M, Ichinose H, Togari A (2000) Changes in cytokines and neurotrophins in Parkinson's disease. *Neural Transm Suppl* 60:277-290

Oh LY, Larsen PH, Krekoski CA, Edwards DR, Donovan F, Werb Z, Yong VW (1999) Matrix metalloproteinase-9/gelatinase B is required for process outgrowth by oligodendrocytes. *J Neurosci* 19:8464-8475

Ouchi Y, Yoshikawa E, Sekine Y, Futatsubashi M, Kanno T, Ogusu T, Torizuka T (2005) Microglial activation and dopamine terminal loss in early Parkinson's disease. *Ann Neurol* 57:168-175

Ouchi Y, Yagi S, Yokokura M, Sakamoto M (2009) Neuroinflammation in the living brain of Parkinson's disease. *Parkinsonism Relat Disord Suppl* 3:S200-204

Page-McCaw A, Ewald AJ, Werb Z (2007) Matrix metalloproteinases and the regulation of tissue

remodelling. *Nat Rev Mol Cell Biol* 8:221-233

Parks WC, Wilson CL, Lopez-Boado YS (2004) Matrix metalloproteinases as modulators of inflammation and innate immunity. *Nat Rev Immunol* 4:617-629

Pott Godoy MC, Tarelli R, Ferrari CC, Sarchi MI, Pitossi FJ (2008) Central and systemic IL-1 exacerbates neurodegeneration and motor symptoms in a model of Parkinson's disease. *Brain* 131:1880-1894

Rolls A, Shechter R, Schwartz M (2009) The bright side of the glial scar in CNS repair. *Nat Rev Neurosci* 10:235-241

Sbai O, Ould-Yahoui A, Ferhat L, Gueye Y, Bernard A, Charrat E, Mehanna A, Risso JJ, Chauvin JP, Fenouillet E, Rivera S, Khrestchatisky M (2010) Differential vesicular distribution and trafficking of MMP-2, MMP-9, and their inhibitors in astrocytes. *Glia* 58:344-366

Sternlicht MD, Werb Z (2001) How matrix metalloproteinases regulate cell behaviour. *Annu Rev Cell Dev Biol* 17:463-516

Streit WJ, Kreutzberg GW (1987) Lectin binding by resting and reactive microglia. *J Neurocytol* 16:249-60

Streit WJ, Walter SA, Pennell NA (1999) Reactive microgliosis. *Progr Neurobiol* 57:563-581

Tansey MG, Goldberg MS (2010) Neuroinflammation in Parkinson's disease: its role in neuronal death and implication for therapeutic intervention. *Neurobiol Dis* 37:510-518

Uhm JH, Dooley NP, Oh LY, Yong VW (1998) Oligodendrocytes utilize a matrix metalloproteinase, MMP-9, to extend processes along an astrocyte extracellular matrix. *Glia* 22:53-63

- Walker EJ, Rosenberg GA (2010) Divergent role for MMP-2 in myelin breakdown and oligodendrocyte death following transient global ischemia. *J Neurosci Res* 88:764-73
- Walsh S, Finn DP, Dowd E (2011) Time-course of nigrostriatal neurodegeneration and neuroinflammation in the 6-hydroxydopamine-induced axonal and terminal lesion models of Parkinson's disease in the rat. *Neuroscience* 175:251-261
- Whitton PS (2010) Neuroinflammation and the prospects for anti-inflammatory treatment of Parkinson's disease. *Curr Opin Investig Drugs* 11:788-794
- Wilczynski GM, Konopacki FA, Wilczek E, Lasiecka Z, Gorlewicz A, Michaluk P, Wawrzyniak M, Malinowska M, Okulski P, Kolodziej LR, Konopka W, Duniec K, Mioduszevska B, Nikolaev E, Walczak A, Owczarek D, Gorecki DC, Zuschratter W, Ottersen OP, Kaczmarek L (2008) Important role of matrix metalloproteinase 9 in epileptogenesis. *J Cell Biol* 180:1021-1035
- Woo MS, Park JS, Choi IY, Kim WK, Kim HS (2008) Inhibition of MMP-3 or -9 suppresses lipopolysaccharide-induced expression of proinflammatory cytokines and iNOS in microglia. *J Neurochem* 106:770-780
- Wright JW, Harding JW (2009) Contributions of matrix metalloproteinases to neural plasticity, habituation, associative learning and drug addiction. *Neural Plast* 2009:579382
- Yong VW (2005) Metalloproteinases: mediators of pathology and regeneration in the CNS. *Nat Rev Neurosci* 6:931-944
- Zhang H, Adwanikar H, Werb Z, Noble-Haeusslein LJ (2010) Matrix metalloproteinases and neurotrauma: evolving roles in injury and reparative processes. *Neuroscientist* 16:156-170

FIGURE LEGENDS

Fig. 1. MMP-9 mRNA and protein levels increase in both substantia nigra (SN) and striatum after MPTP treatment. **a, b** MMP-9 mRNA levels in control and MPTP-treated mice. MMP-9 mRNA levels increase significantly, compared to control (Cntr), within 24 h after the last MPTP injection in both SN (**a**) and striatum (**b**). However, while in the SN we observe a further increase after 48 h and then a decrease towards Cntr levels, in the striatum MMP-9 mRNA decreases significantly below Cntr, until the 2 weeks (w) time point. $n = 8$ mice/experimental group. Data are represented as the mean \pm s.e.m. of mRNA levels in MPTP-treated mice/control. **c-d'** MMP-9 Western immunoblot and relative quantitative analysis in control and MPTP-treated mice. **c-d** Typical MMP-9 Western immunoblot in the SN (**c**) and striatum (**d**). MMP-9 antibody recognized two bands at the predicted molecular mass of the pro- (100 kDa) and active (92 kDa) MMP-9. The recombinant human MMP-9 used as standard (St) migrates at a slightly lower molecular mass respect to the mouse active MMP-9. GAPDH was used as the internal reference protein. **c', d'** Densitometric analyses of the immunopositive bands reveals an early and significant increase, compared to control, in the protein levels of both pro- and active MMP-9, 24 h (SN) and 1 h (striatum) after MPTP injection. Protein levels remain significantly higher than control throughout the post-injection time considered. O.D.: optical density. $n = 8$ animals/experimental group. Data are represented as the mean \pm s.e.m. of O.D. in MPTP-treated mice/control. $*p \leq 0.05$, calculated by one-way ANOVA and Duncan's test.

Fig. 2. Gelatinolytic activity increases in the SN and striatum of MPTP-treated mice compared to control. Representative brain cryosections showing an increase, respect to control, in both number of labeled cells and intensity of the fluorescent signal of MMP-9 gelatinolytic activity after MPTP treatment, obtained by *in situ* zymography. Lines are to guide the eye in SN demarcation. Scale bar: 100 μ m.

Fig. 3. MMP-9 is mainly neuronal in both control and MPTP-treated mice, but the number of immunopositive neurons is differently modulated along the nigro-striatal pathway. Confocal images of MMP-9 co-immunolabeling with NeuN and TH in the substantia nigra *pars compacta* (SN_{pc}) and striatum of control and MPTP-treated mice (72 h after MPTP injection) and relative quantitative analyses. **a** MMP-9 (green) co-localizes with both NeuN (purple) and TH (red) in SN_{pc} sections of control and parkinsonian mice. MMP-9 largely localizes in dopaminergic neurons, labeling both cell bodies and axons (arrow in the merge panel). However, the few non-dopaminergic neurons present in the SN_{pc} are also immunopositive (arrowhead in the merge panel). Nuclei are stained in blue with DAPI. Scale bar: 25 μ m. **a'** The number of MMP-9⁺ (black bars), NeuN⁺ (gray bars) and NeuN⁺/MMP-9⁺ (white bars) cells undergo a significant decrease, respect to control (Cntr), 24 h after MPTP treatment, followed by a partial, but significant recovery (respect to the 72 h time point) after 2 weeks (w). **a''** The number of TH⁺ (black bars), TH⁺/MMP-9⁺ (gray bars) cells follows the same time course described for the SN. Differently, the number of NeuN⁺/TH⁻ (white bars) does not change and that of NeuN⁺/MMP-9⁺/TH⁻ (white-black bars) cells increases slightly, but significantly, 72 h after MPTP treatment. **b** MMP-9 (green) largely co-localizes with NeuN (purple) in sections of striatum from control and parkinsonian mice (arrows in the enlarged boxed area), although not all neurons are MMP-9⁺ (arrowhead in the enlarged boxed area). Nuclei are stained in blue with DAPI. Scale bar: low magnification, 40 μ m; enlarged boxed area, 10 μ m. **b'** The number of MMP-9⁺ cells (black bars) increase significantly respect to Cntr by 48 h after MPTP injection, remaining higher up to 2 w. Differently, the number of neurons, either expressing MMP-9 (NeuN⁺/MMP-9⁺) (white bars) or not (NeuN⁺) (gray bars) does not change. n = 4 animals/experimental group. For all quantitative analyses, data are represented as the mean \pm s.e.m. of the cell number/mm². *p \leq 0.05 (MPTP vs Cntr); ^p \leq 0.05 (2 w vs 72 h MPTP) calculated by one-way ANOVA and Duncan's test.

Fig. 4. Time course of the changes in TH protein levels in both substantia nigra (SN) and striatum of MPTP-treated mice. **a, b** Typical Western immunoblots revealing levels of TH on protein extracts from the SN (**a**) and striatum (**b**) of control (Cntr) and MPTP-treated mice, from 1 h to 2 weeks (w) post-injection. The anti-TH antibody recognizes a single band of about 62 kDa. The intensity of the band decreases after MPTP treatment, respect to Cntr, and partially recover after 2 w. GAPDH is used as the internal reference protein. Molecular mass standards, expressed in kDa, are indicated on the right hand side. **a', b'** Densitometric analysis reveals a significant decrease in TH protein levels by 24 h (striatum)-48 h (SN), which remain lower than control until the last time point examined. However, a partial recovery, more evident in the SN, is observed after 2 w. O.D: optical density. n = 8 mice/experimental group. Data are represented as the mean \pm s.e.m. of O.D. of the immunopositive bands. * $p \leq 0.05$, calculated by one way ANOVA and Duncan's test.

Fig. 5. MMP-9 expression by microglia and astrocytes significantly increase soon after MPTP treatment, concomitantly with a massive inflammatory response. Confocal study of MMP-9 co-labeling with GSA and GFAP in the substantia nigra *pars compacta* (SN_{pc}) and striatum of control and MPTP-treated mice and relative quantitative analyses. **a** In the SN_{pc} of control mice, GSA (red) staining labeled microglia cell bodies and thin processes (arrowheads). MMP-9/GSA co-localization is practically absent. Seventy-two hours after MPTP treatment, an activated phenotype is recognizable, with increased cell size. Labeling with MMP-9 (green), denotes some punctiform co-localization (arrows and enlarged boxed area). Nuclei are counterstained with DAPI (blue). Scale bars: 20 μ m; enlarged boxed area, 25 μ m. **a'** Quantitative analysis shows that a very few of the MMP-9⁺ cells (black bars) are also GSA⁺ (white bars), in both control (Cntr) and MPTP-treated mice. However, while the number of MMP-9⁺ cells significantly decreases respect to Cntr after MPTP injection, that of GSA⁺ (gray bars) and of GSA⁺/MMP-9⁺ microglial cells increases by 24 h and 48 h, respectively. These values decrease significantly, respect to the 72 h time point, after 2 weeks (w). **b** Representative confocal images of double-immunolabeling of MMP-9 (green) and GFAP (red) in the SN_{pc} of both control and MPTP-treated animals. As for microglia, in control

animals, astrocytes are little and dispersed (arrowheads). Seventy-two hours after MPTP treatment, a prominent astrogliosis is evident, with increase in cell size, number and length of cell processes. MMP-9 and GFAP co-localized in part (arrows and enlarged boxed area). Nuclei are counterstained with DAPI (blue). Scale bars: 20 μm ; enlarged boxed area, 25 μm . **b'** Quantitative analysis of GFAP⁺ (gray bars) and GFAP⁺/MMP-9⁺ cells (white bars) show a significant increase in the number of labeled cells by 24 h after MPTP treatment respect to Cntr. Both values decrease significantly at the end of the post-operative time considered, when the GFAP⁺ cell number returns similar to Cntr. **c, d** Quantitative analysis of MMP-9⁺ cells alone (black bars) or in co-localization with GSA (white bars in **c**) and GFAP (white bars in **d**) in the striatum. MMP-9⁺ cells increase significantly, respect to control, after MPTP treatment, remaining high up to the 2 w time point. Also the number of both microglia (GSA⁺ cells, gray bars in **c**) and astrocytes (GFAP⁺ cells, gray bars in **d**), increases. After 2 w, GSA⁺ cells and GFAP⁺/MMP-9⁺ cells decrease significantly respect to the previous time point, while the number of GSA⁺/MMP-9⁺ and GFAP⁺ cells remains similar. For all quantitative analyses, n = 4 animals/experimental group. Data are represented as the mean \pm s.e.m. of the cell number/mm². *p \leq 0.05 (MPTP vs Cntr), ^p \leq 0.05 (2 w vs 72 h MPTP) calculated by one-way ANOVA and Duncan's test.

Fig. 6. Pie charts resuming the changes in the number of the different cell types expressing MMP-9 in the mouse SNpc and striatum. MMP-9 is mainly expressed by neurons in both SNpc (left column) and striatum (right column). The percentage of MMP-9⁺ neurons decreases significantly after MPTP treatment, in coincidence with dopaminergic neuron loss and neuroinflammation (24 h-72 h), whereas that of MMP-9⁺ microglia, astrocytes and other types of cells increases. Two weeks after MPTP treatment, percentages return similar to control.

Fig. 7. MMP-9 expression in neurons and astrocytes significantly increases in the caudate and putamen of parkinsonian *Macaca fascicularis*, coinciding with a chronic and massive neuroinflammation. Confocal study of MMP-9 co-immunolabeling with NeuN and GFAP in the

caudate and putamen of control and MPTP-treated monkeys and relative quantitative analyses. **a** MMP-9 immunofluorescence (green) decorates the cell bodies of numerous cells, mainly with a glial morphology. Co-localization of MMP-9 and NeuN (purple) (arrows and enlarged boxed areas) increase after two years of stable Parkinsonism. Nuclei are counterstained with DAPI (blue). Scale bars: 25 μm . **a'** Quantitative analysis of MMP-9⁺ (black bars), NeuN⁺ (gray bars) and NeuN⁺/MMP-9⁺ (white bars) cells indicate a significant increase, respect to control (Cntr), in the number of cells expressing MMP-9, including neurons, after induction of stable parkinsonism in both caudate and putamen. Differently, the number of striatal neurons remains unchanged. **b** Co-immunolabeling of MMP-9 (green) and GFAP (red) shows a clear astrogliosis after MPTP treatment. A number of cells and processes are immunolabeled with both markers (arrows and enlarged boxed areas). Nuclei are stained with DAPI (blue). Scale bars: 25 μm . **b'** Quantitative analysis of MMP-9⁺ (black bars), GFAP⁺ (gray bars) and GFAP⁺/MMP-9⁺ (white bars) cells show a significant increase, respect to control, in the number of astrocytes, expressing or not MMP-9, in both caudate and putamen. $n = 3$ monkeys (control) and 5 monkeys (Parkinsonian). For all quantitative analyses, data are represented as the mean \pm s.e.m. of cell number/ mm^2 . * $p \leq 0.05$, ** $p \leq 0.01$, *** $p \leq 0.001$ calculated by the Student's t test.

Fig. 8. After MPTP treatment, the amount of dopaminergic neurons and fibers in the substantia nigra *pars compacta* (SN_{pc}) and striatum is significantly higher in MMP-9 KO mice respect to wild-type. **a** TH immunohistochemistry in the SN_{pc} of both wild-type and MMP-9 KO mice shows a decrease (72 h) of the immunolabeling after MPTP treatment respect to control. This reduction partially recovers after 2 weeks (w) from the treatment. Scale bar: 400 μm . **b** Quantitative analysis of the number of TH⁺ cells (expressed as the percentage respect to their own control) confirms this pattern and shows that the number of dopaminergic neurons expressing TH is always significantly higher in the KO genotype (black bars) respect to wild-type (white bars). Partial, but significant, retrieval of TH⁺ neurons at the 2 w time point indicates that a number of dopaminergic neurons

survive MPTP intoxication and recover their functionality. **c** Quantitative analysis of the changes of SNpc neurons, stained with the histological dye cresyl violet, was performed to ascertain neuronal loss respect to TH-expressing neurons. Data demonstrate effective and definitive loss of a percentage of neurons after MPTP treatment in both genotypes (without recovery after 2 w). The number of lost neurons was always significantly higher in wild-type mice (white bars) respect to MMP-9 KO (black bars). **d** As for the SNpc, TH immunostaining of striatal sections shows an evident decrease (72 h) and successive partial recovery (2 w) of immunolabeling after MPTP treatment respect to control, in both wild-type and MMP-9 KO mice. Scale bar: 1 mm. **e** Densitometric analysis of the immunopositive signal confirms a significant drastic decrease in TH immunolabeling 72 h after MPTP treatment and a significant recovery after 2 w. n = 5 mice (wild-type) and 8 mice (MMP-9 KO). For all quantitative analyses, data are represented as the mean \pm s.e.m. of the number of neurons (**b, c**) and of the O.D. in MPTP-treated mice/control (**e**). *p \leq 0.05, ***p \leq 0.001 (MPTP vs Cntr), #p \leq 0.05, ###p \leq 0.001 (MMP-9 KO vs wild-type mice), ^p \leq 0.05, ^^p \leq 0.001 (2 w vs 72h MPTP), calculated by the Student's *t* test.

Fig. 9. MPTP treatment induces a prominent microgliosis in the substantia nigra *pars compacta* (SNpc) and striatum of both wild-type and MMP-9 KO mice, but the mean cell size is significantly reduced in the KO genotype. **a, d** Iba-1 immunohistochemistry in the SNpc (**a**) and striatum (**d**) of both wild-type and MMP-9 KO mice shows an increase, respect to control, in the amount of clusters of reactive microglia 72 h after MPTP treatment. After 2 weeks (w), number and size of microglial cells begin to reduce respect to the 72 h post-injection time. Insets show details of microglia morphology, before and after MPTP treatment. Insets in panel **a** (SNpc): **a**¹ and **a**³ are enlargements of microglial cells in control wild-type and MMP-9 KO mice, respectively; **a**² and **a**⁴ are enlargements of microglial cells 72 h after MPTP treatment of wild-type and MMP-9 KO mice, respectively. Scale bars: **a**, 400 μ m; **d**, 200 μ m; **insets**, 20 μ m. **b, e** Quantitative analysis on Iba-1⁺ cells in the SNpc and striatum of wild type and MMP-9 KO mice shows that the number of microglial cells increases significantly 72 h after MPTP treatment and begins to decrease after 2 w,

although remaining higher than control (Cntr). No differences are observed between the two genotypes. Data are represented as the mean \pm s.e.m. of the cell number/photographic field. **c,f** Quantitative analysis on Iba-1⁺ cells in the SNpc and striatum of wild type and MMP-9 KO mice shows that the mean area occupied by each microglial cell significantly increases 72 h after MPTP treatment, respect to Cntr, and then decreases after 2 w. However, in MMP-9 KO mice, this parameter is significantly lower compared to wild-type, at least after 72 h. n = 5 mice (wild-type) and 8 mice (MMP-9 KO). For all quantitative analyses, data are represented as the mean \pm s.e.m. of cell area (μm^2); *p \leq 0.05, **p \leq 0.01, ***p \leq 0.001 (MPTP vs Ctrl); ^p \leq 0.05, ^^p \leq 0.001 (2 w vs 72 h MPTP); #p \leq 0.05, ##p \leq 0.01 (MMP-9 KO vs wild-type), calculated by the Student's *t* test.

Fig. 10. MPTP treatment induces a prominent astrogliosis in the substantia nigra *pars compacta* (SNpc) and striatum of both wild-type and MMP-9 KO mice, but the mean cell size is significantly reduced in the KO genotype. **a, d** GFAP immunohistochemistry in the SNpc (**a**) and striatum (**d**) of both wild-type and MMP-9 KO mice shows an increase, respect to control, in the amount of reactive astrocytes 72 h after MPTP treatment. Reactive astrocytes increase cell size and complexity of their processes. After 2 weeks (w), astrocyte number and size begin to reduce respect to the 72 h post-injection time. Insets show details of astrocyte morphology, before and after MPTP treatment. Insets to panel **a** (SNpc): **a**¹ and **a**³ are enlargements of astrocytes in control wild-type and MMP-9 KO mice, respectively; **a**² and **a**⁴ are enlargements of astrocytes 72 h after MPTP treatment of wild-type and MMP-9 KO mice, respectively. Scale bars: **a**, 400 μm ; **d**, 200 μm ; **insets**, 20 μm . **b, e** Quantitative analysis on GFAP⁺ cells in the SNpc and striatum of wild-type and MMP-9 KO mice shows that the number of astrocytes increases significantly 72 h after MPTP treatment and begin to decrease after 2 w, although remaining higher than control (Cntr). No differences are observed between the two genotypes. Data are represented as the mean \pm s.e.m. of the cell number/photographic field. **c, f** Quantitative analysis on GFAP⁺ cells in the SNpc and striatum of wild type and MMP-9 KO mice shows that the mean area occupied by each astrocyte significantly increases 72 h after MPTP treatment, respect to Cntr, and then decreases after 2 w. However, 72 h

after MPTP treatment, this parameter in MMP-9 KO mice is significantly lower compared to wild-type. $n = 5$ mice (wild-type) and 8 mice (MMP-9 KO). For all quantitative analyses, data are represented as the mean \pm s.e.m. of cell area (μm^2); $**p \leq 0.01$, $***p \leq 0.001$ (MPTP vs Ctrl); $^^^p \leq 0.001$ (2 w vs 72 h MPTP); $\#p \leq 0.05$ (MMP-9 KO vs wild-type), calculated by the Student's t test.

Fig. 11. Glial cells activation (neuroinflammation) inversely correlates with the number of TH⁺ cells in the substantia nigra (SN) and levels of TH immunopositivity in the striatum. Increase in the mean cell area (μm^2) occupied by both microglia (Iba-1⁺ cells) and astrocytes (GFAP⁺ cells) inversely correlates to the levels of TH immunostaining in both SNpc and striatum of wild-type mice (black dots and black tendency lines). The inverse correlation is almost lost in the MMP-9 KO mice (red dots and red tendency lines). $n = 15$ mice (wild-type) and 24 mice (MMP-9 KO). P-values, calculated by Pearson correlation coefficient (R^2), are indicated for each graph.

Fig. 12. Synopsis of the response of the nigro-striatal-cortical circuit to acute MPTP intoxication. In the dynamics of the events, the proposed role of MMP-9 in the exacerbation of dopaminergic neuron death and neuroinflammatory response is highlighted. Oligodendrocytes and the hypothesized role they may play in the process of partial recovery of the nigrostriatal pathway are also depicted.

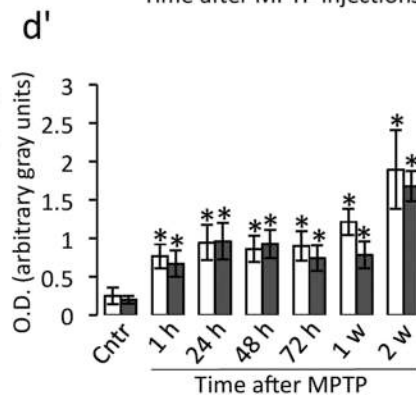
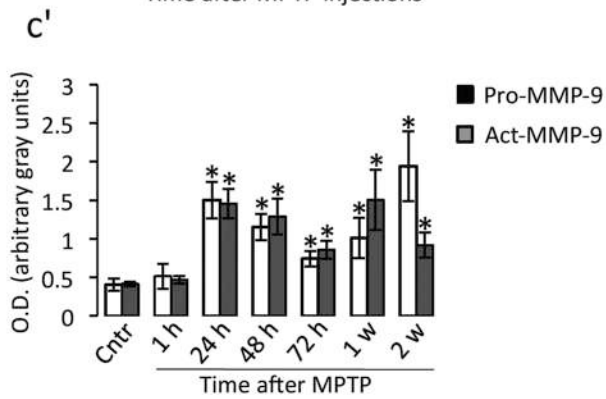
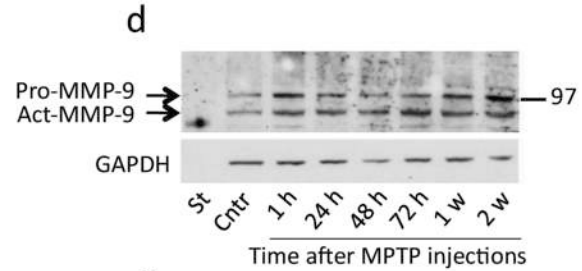
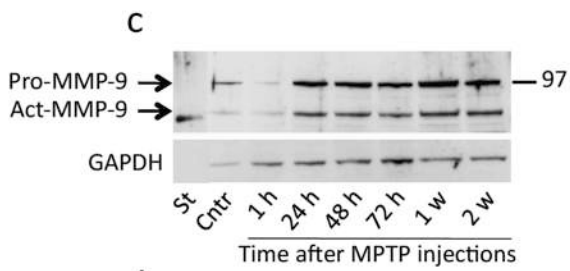
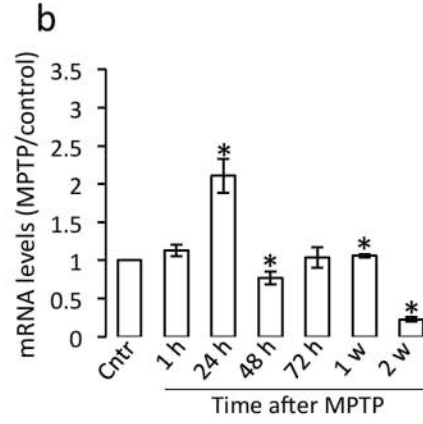
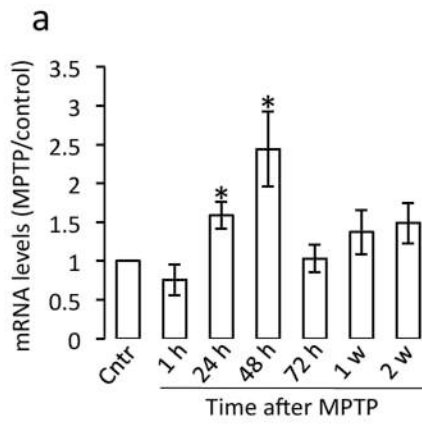
Table 1. Motor score of parkinsonism evaluated for each monkey, cumulative dose of MPTP received and time of survival after the last MPTP administration

Monkey	Sex	Motor Score	MPTP (mg/Kg)	Years after MPTP
C1	M	0.0	0	-
C2	M	0.0	0	-
C3	F	0.0	0	-
P1	M	3.5	1.8	2
P2	F	4.2	0.9	2
P3	M	5.0	1.8	2
P4	F	9.2	0.9	2

C; Control, P; Parkinsonian; M, Male; F, Female

Substantia Nigra

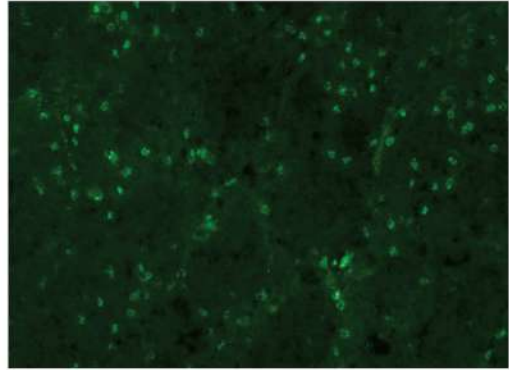
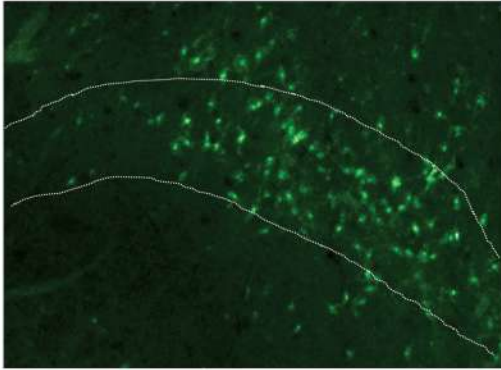
Striatum



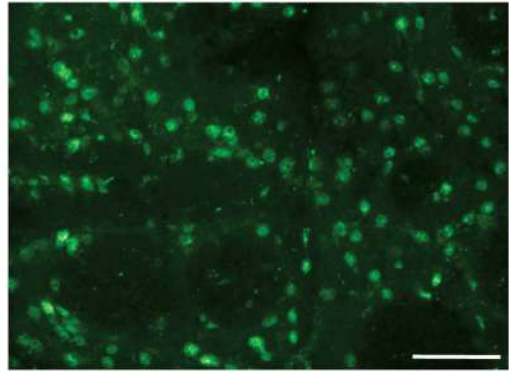
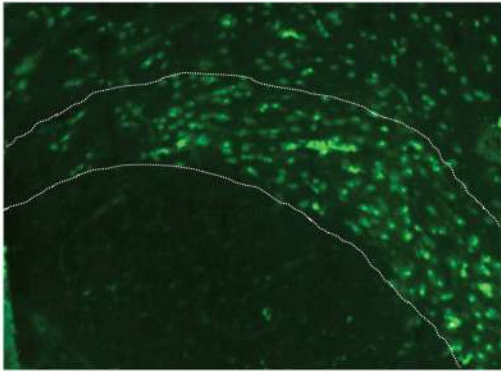
Substantia Nigra

Striatum

Control

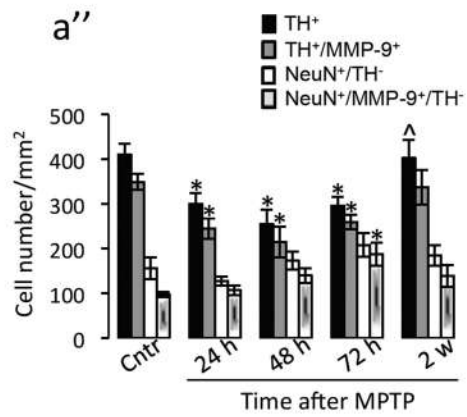
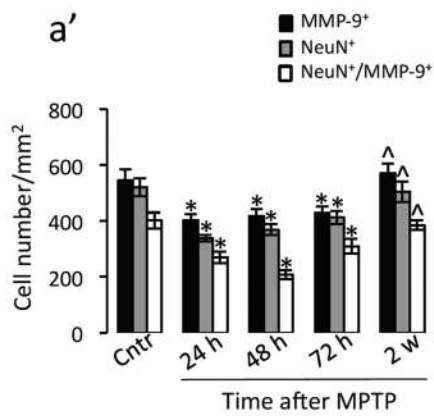
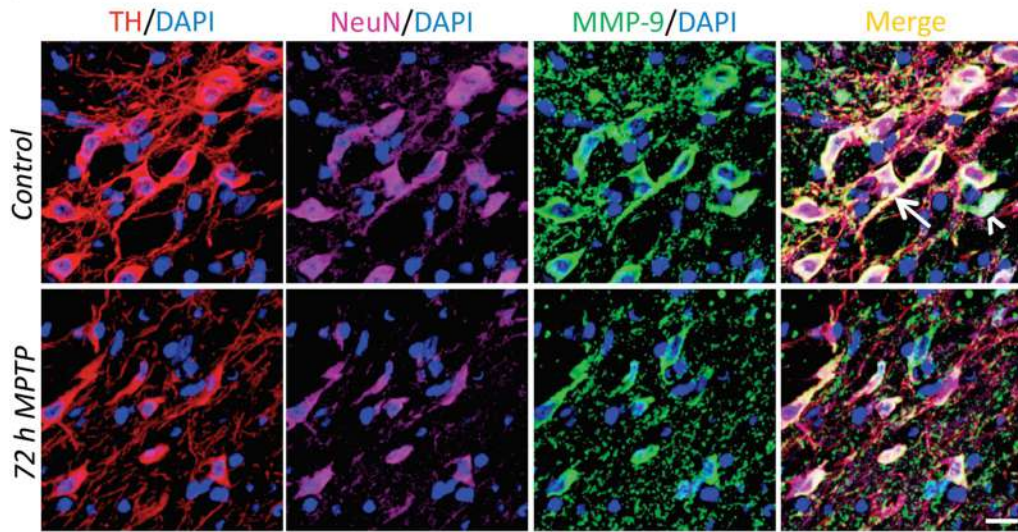


72 h MPTP



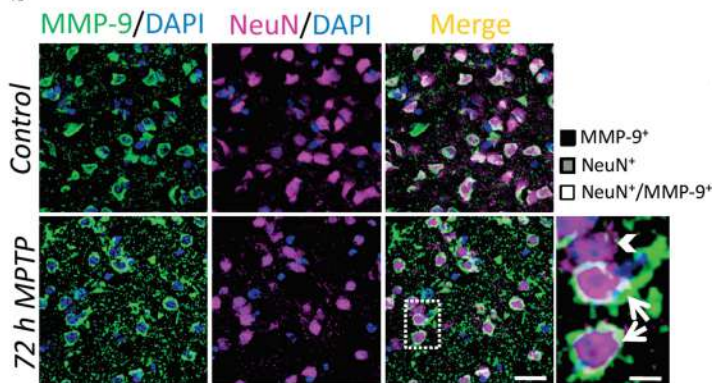
Substantia Nigra

a

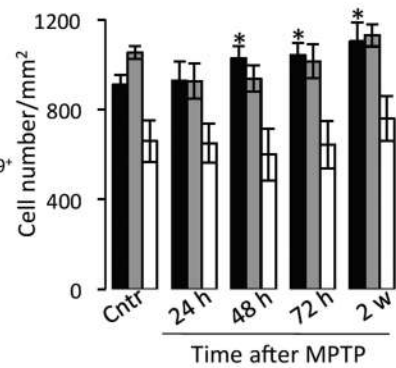


Striatum

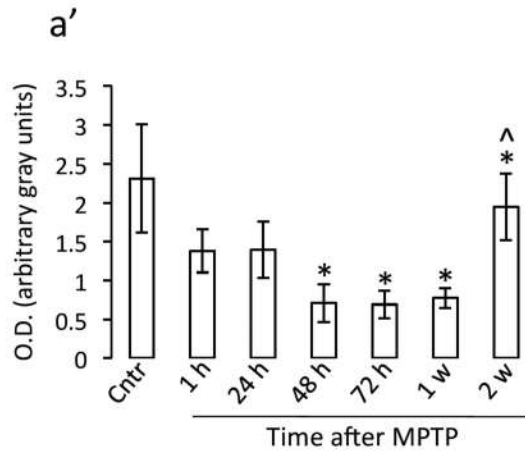
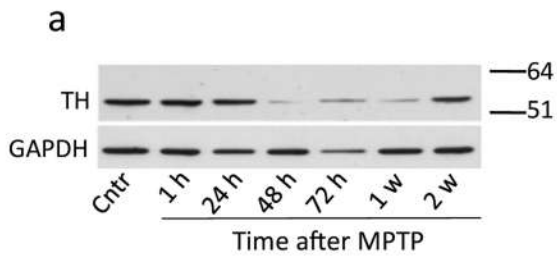
b



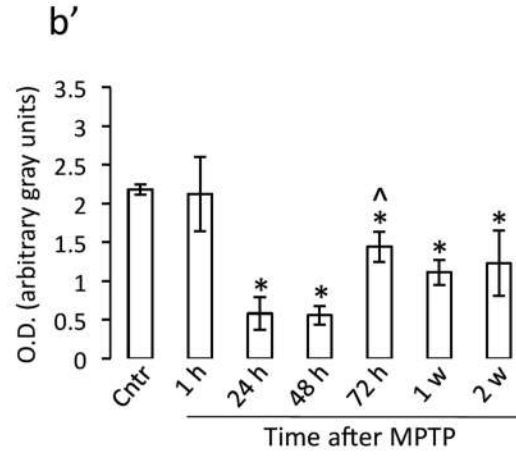
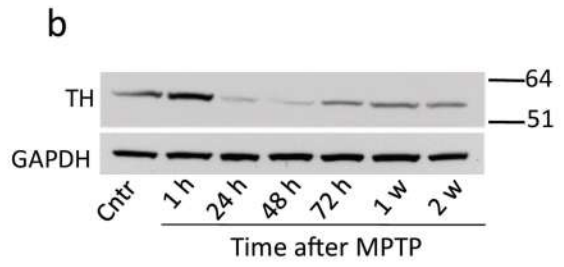
b'



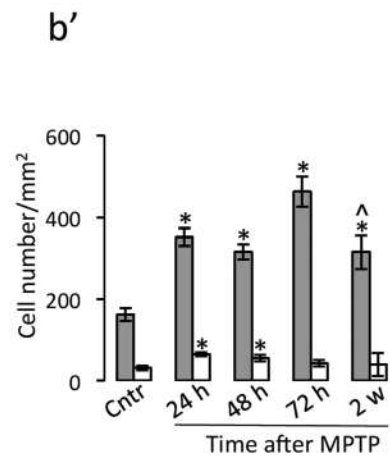
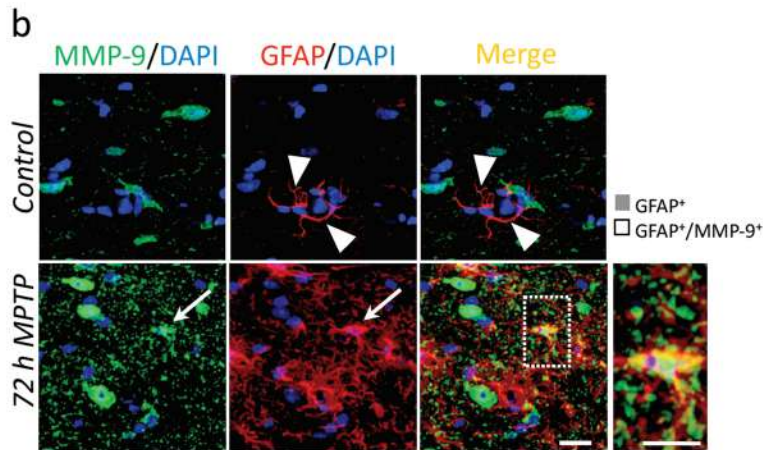
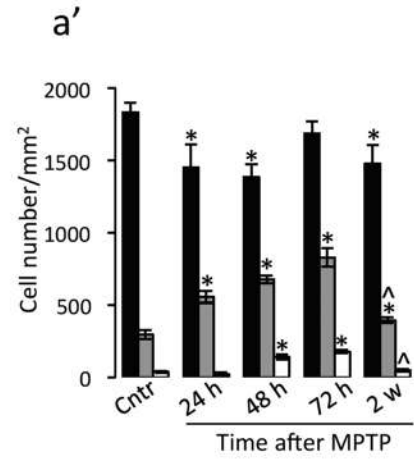
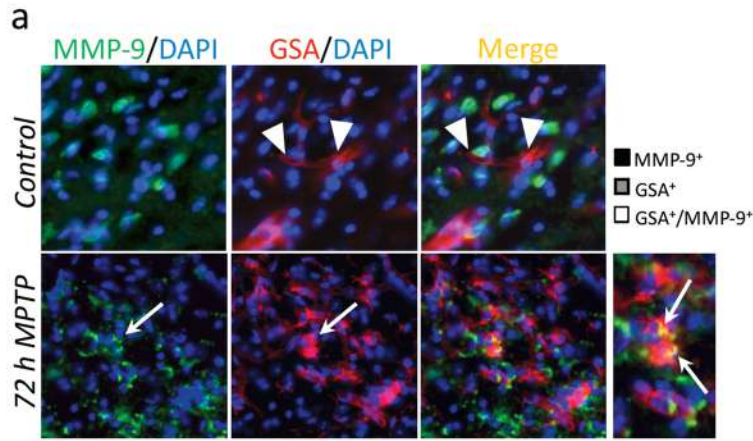
Substantia Nigra



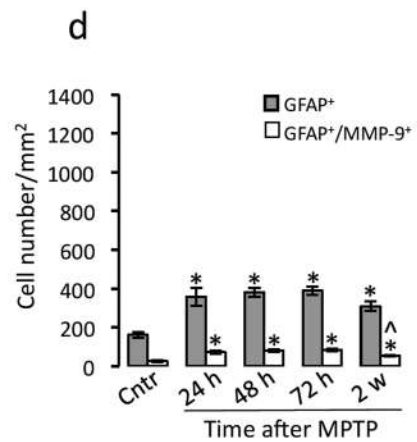
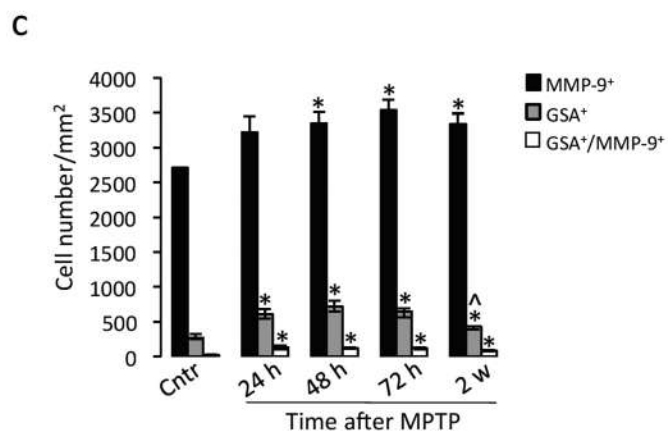
Striatum

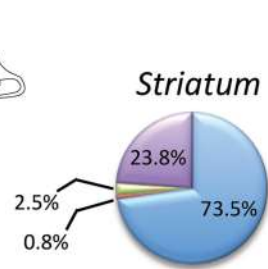
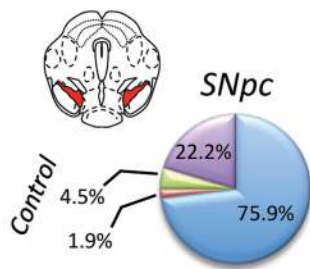


Substantia Nigra

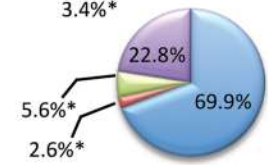
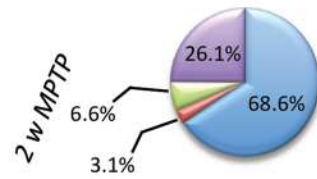
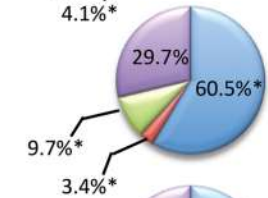
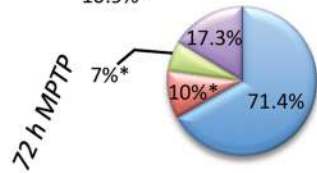
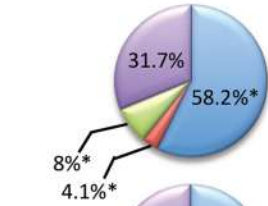
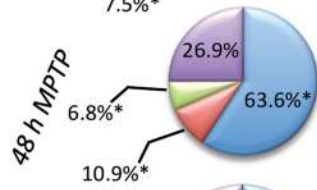
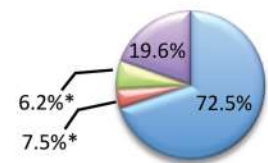
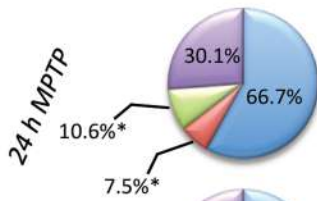


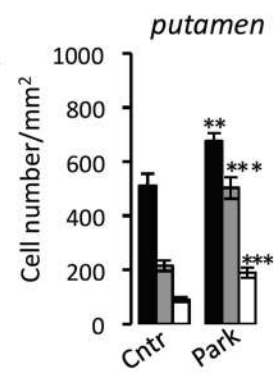
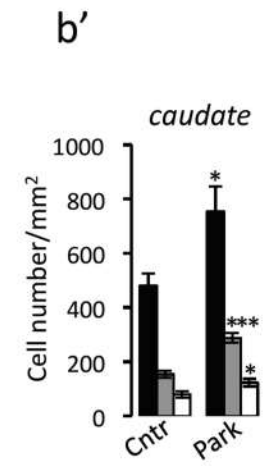
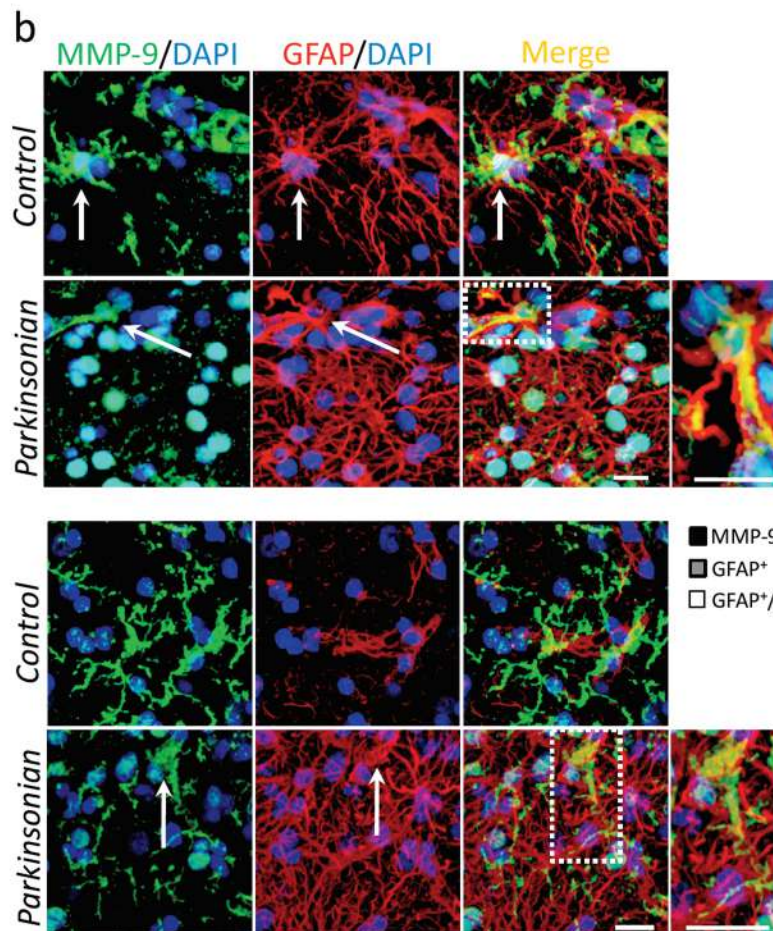
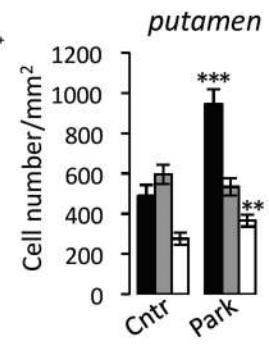
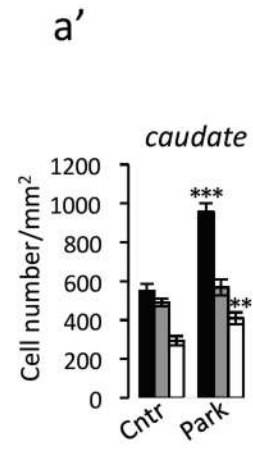
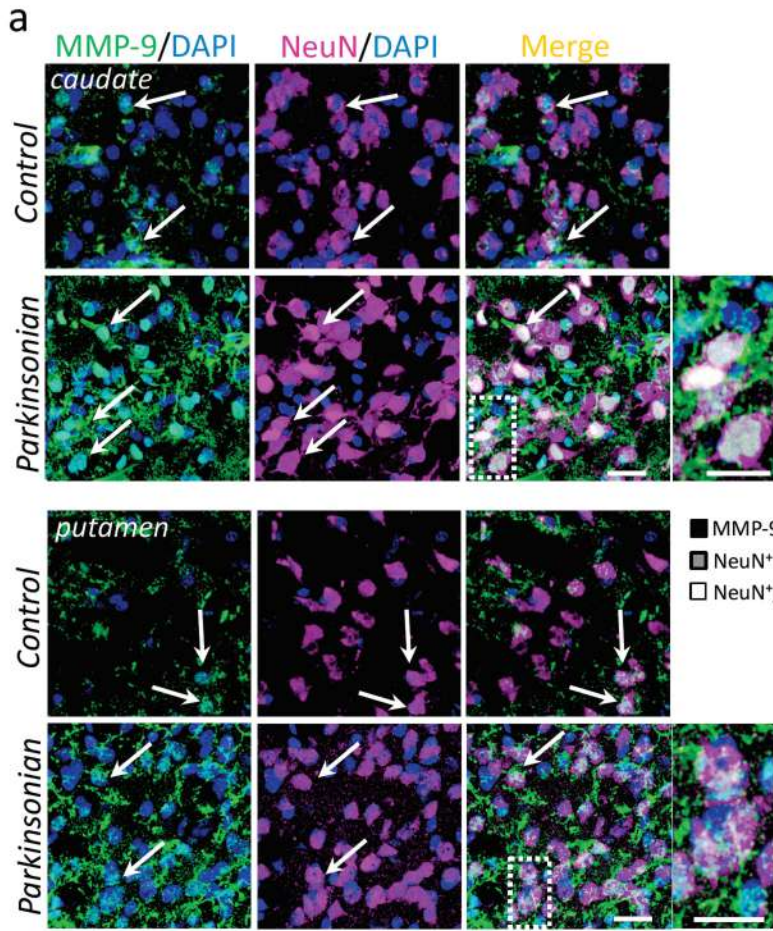
Striatum

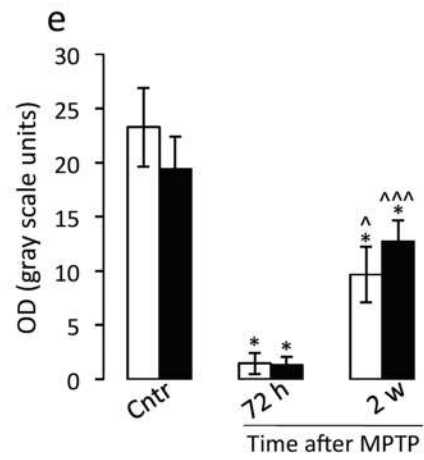
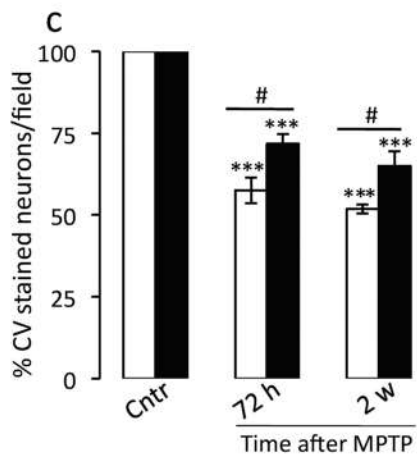
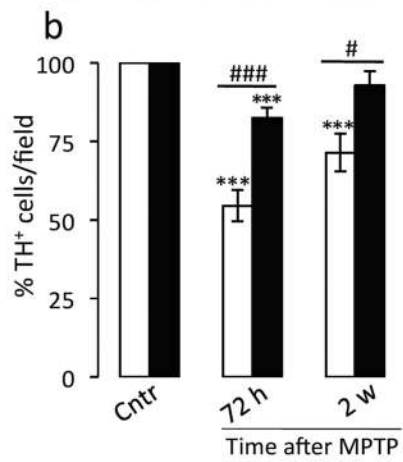
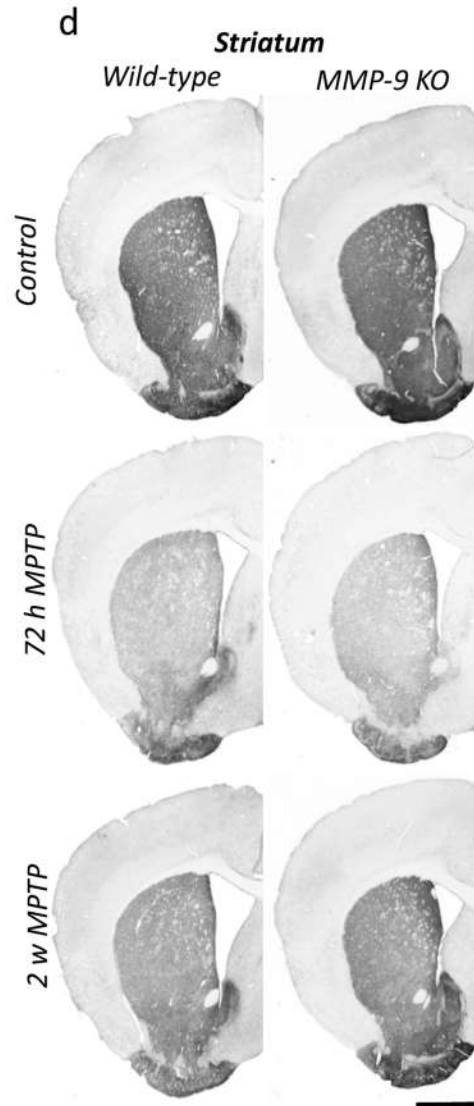
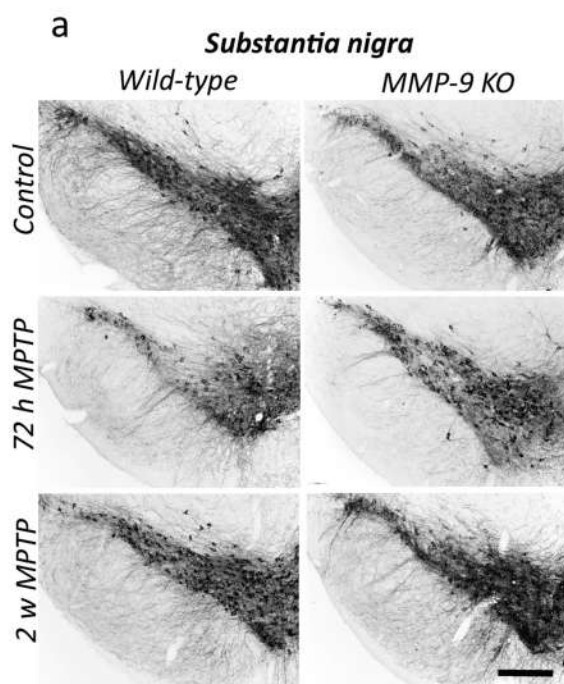


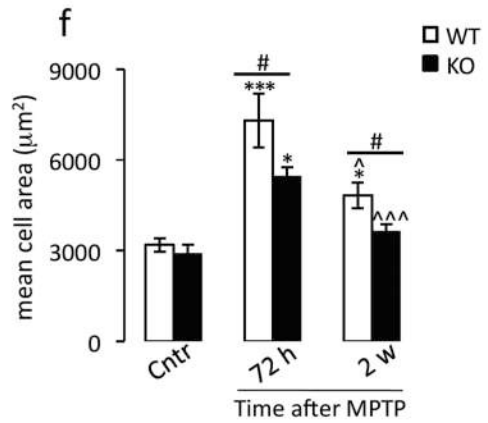
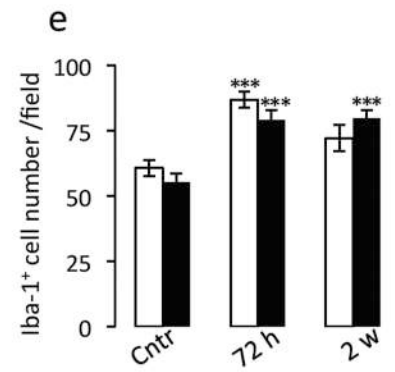
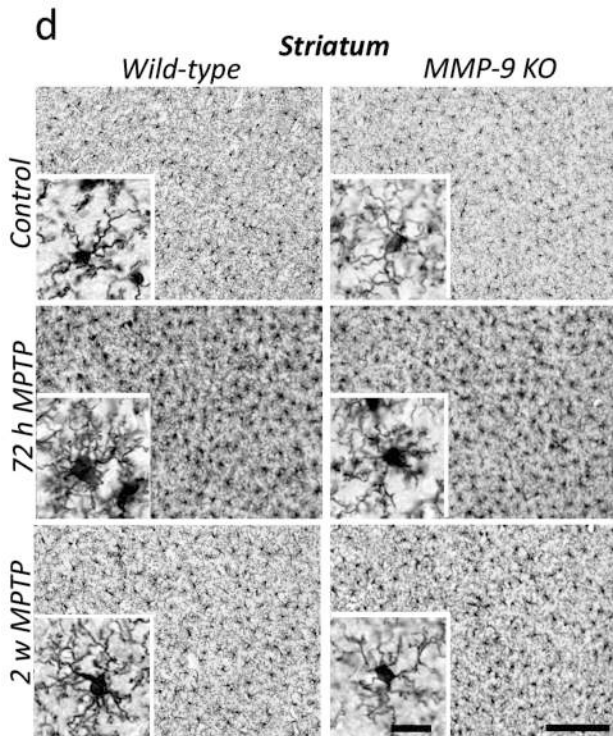
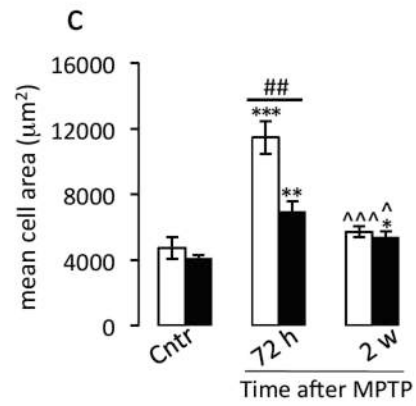
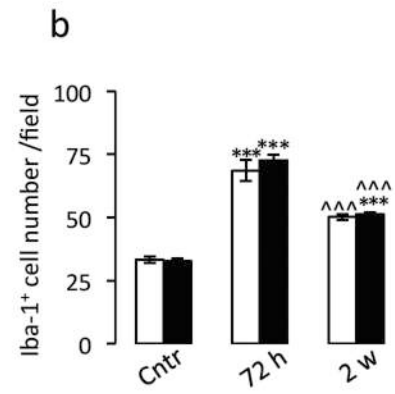
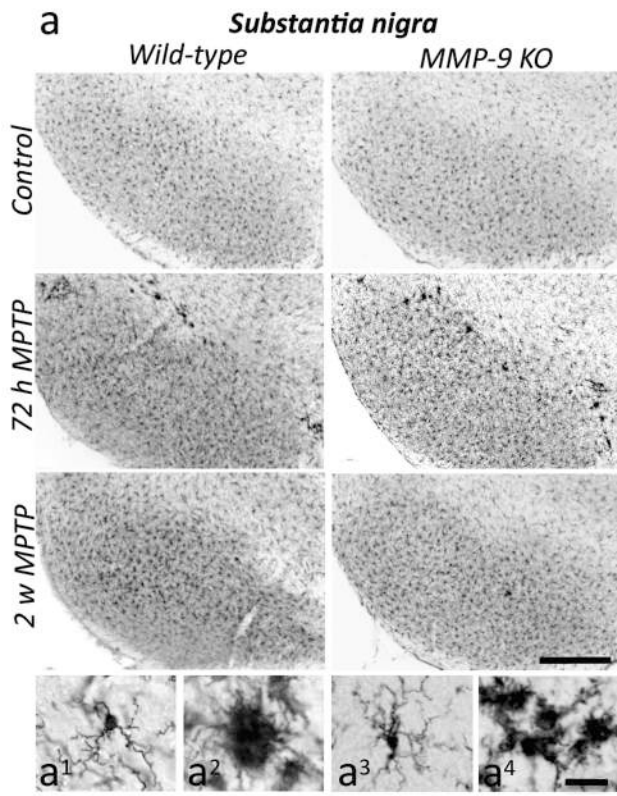


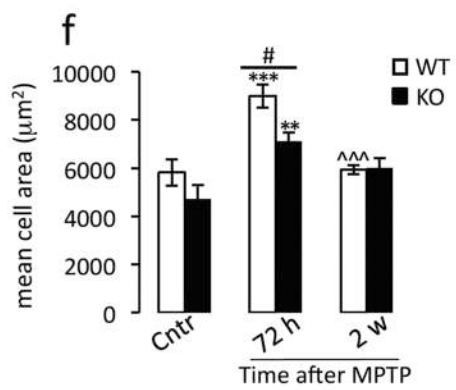
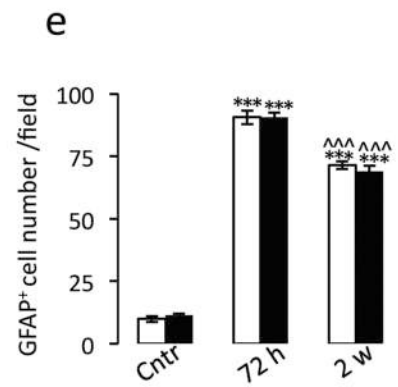
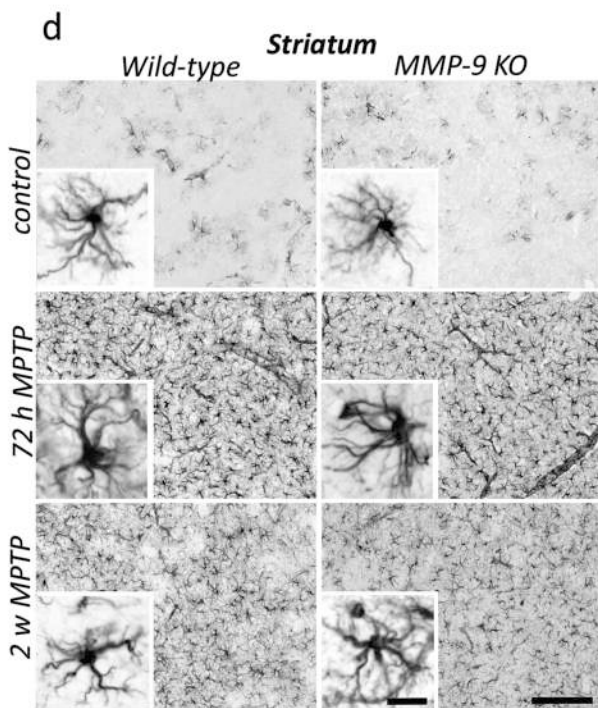
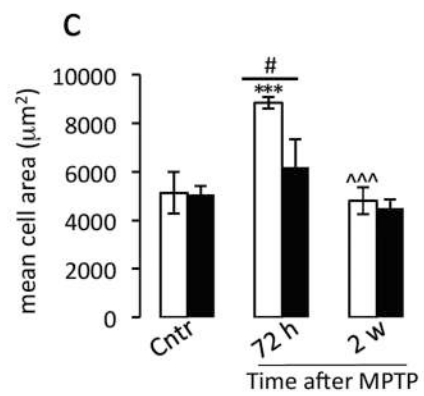
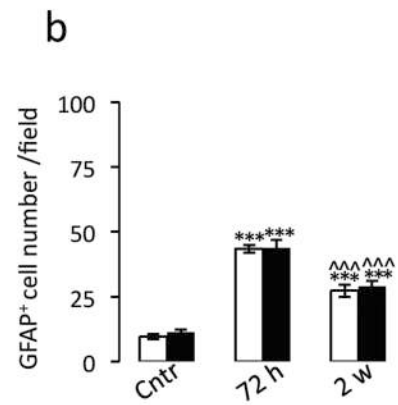
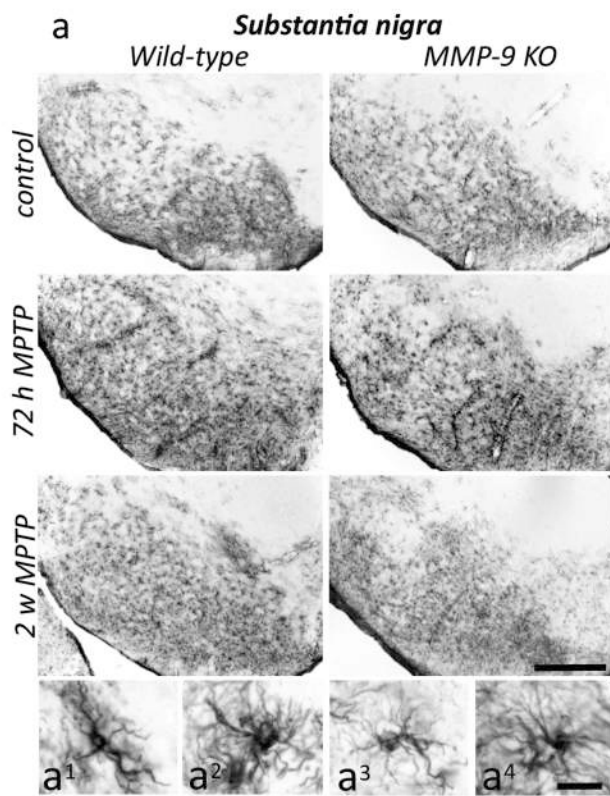
- Neurons
- Microglia
- Astrocytes
- Others





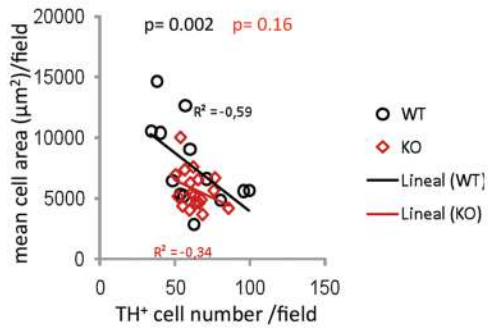




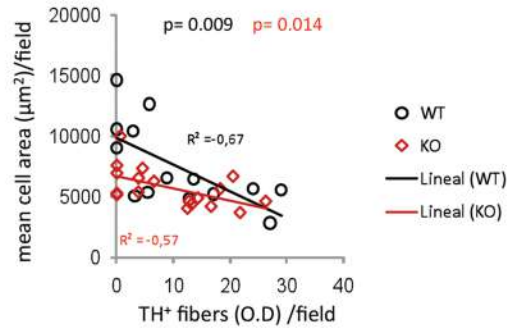


Substantia nigra

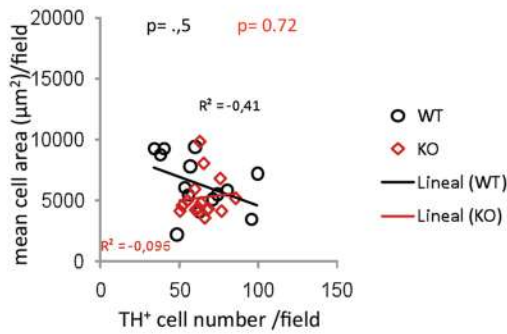
Iba-1⁺ cells



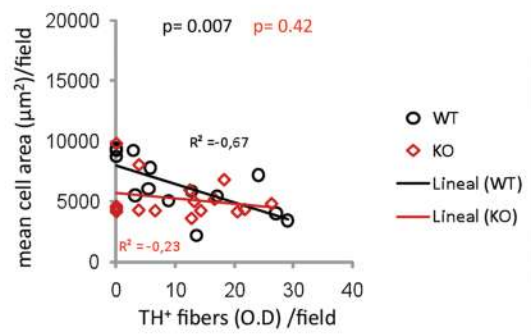
Iba-1⁺ cells



GFAP⁺ cells

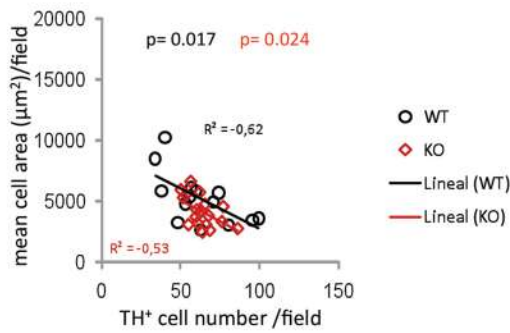


GFAP⁺ cells

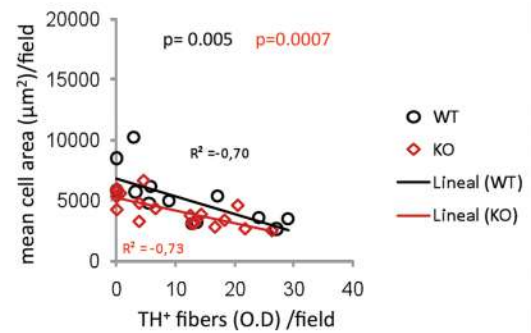


Striatum

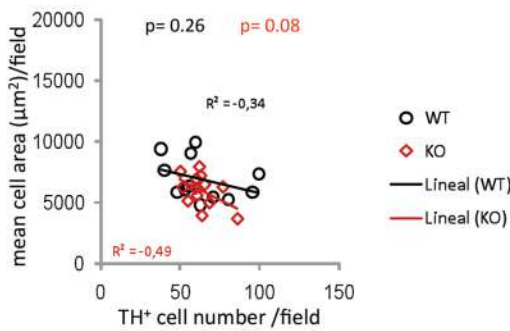
Iba-1⁺ cells



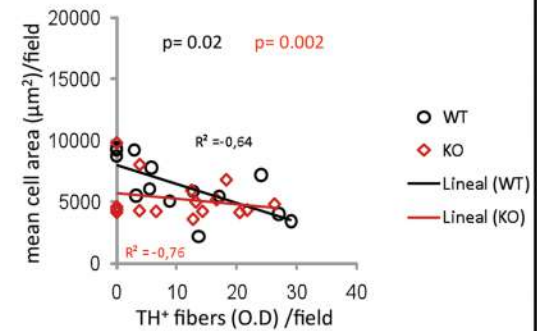
Iba-1⁺ cells

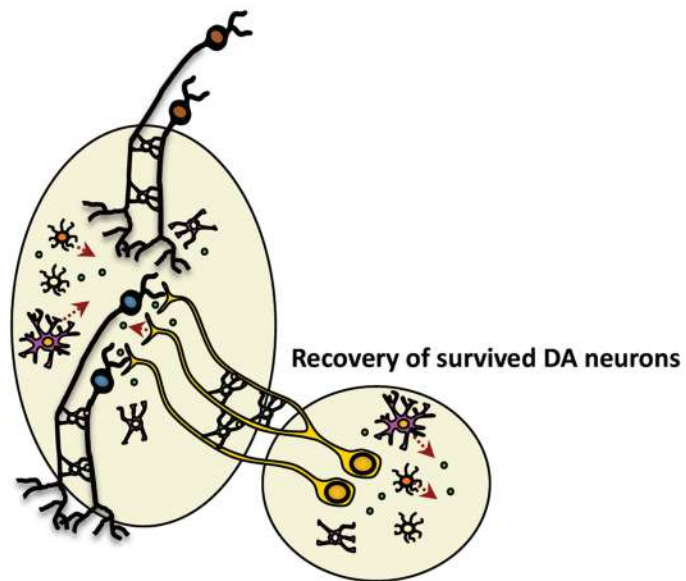
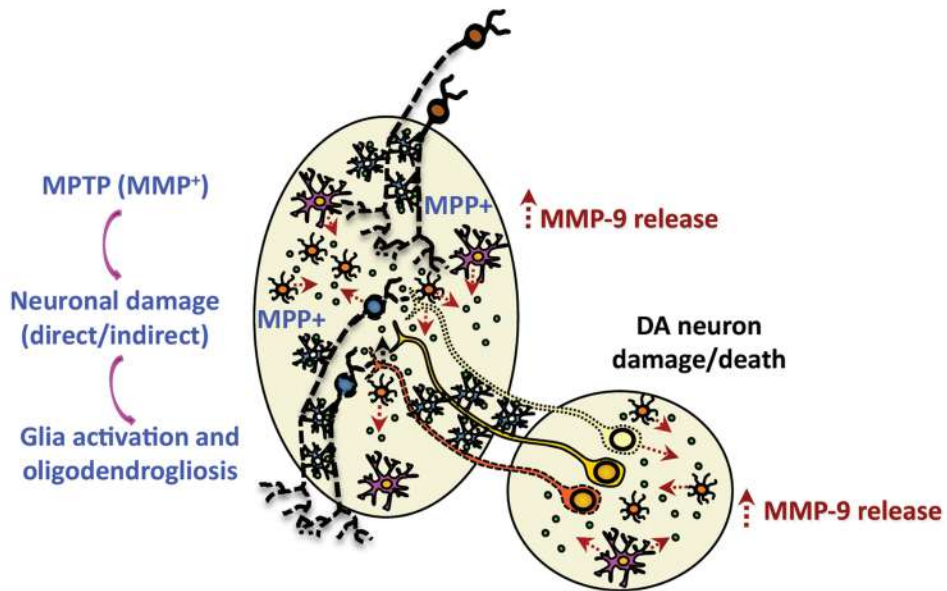
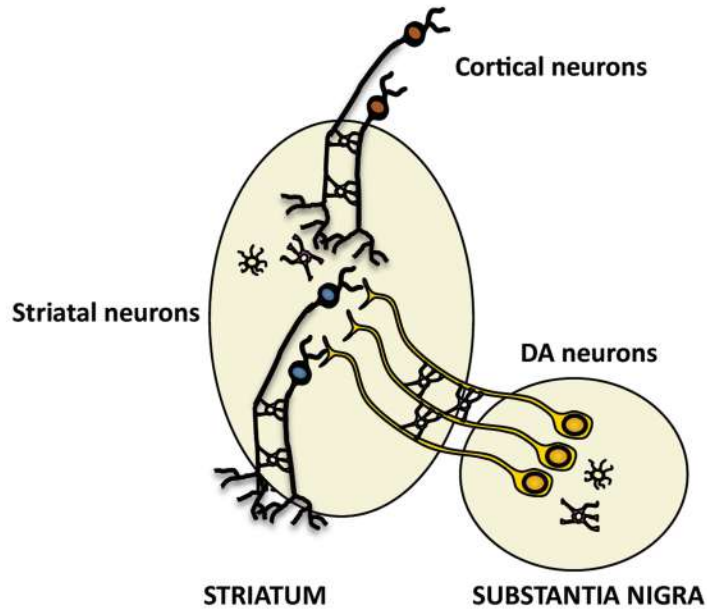









GFAP⁺ cells



GFAP⁺ cells





-  microglia
-  activated microglia
-  astrocyte
-  reactive astrocyte
-  oligodendrocyte
-  reactive oligodendrocyte
-  MMP-9